Applied Energy 377 (2025) 124597

Contents lists available at ScienceDirect

Applied Energy

journal homepage: www.elsevier.com/locate/apenergy

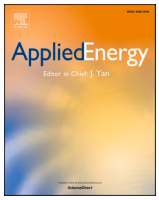

A cooling demand estimator for housing communities in a warming world

Pranaynil Saikia, Lloyd Corcoran, Carlos E. Ugalde-Loo *, Muditha Abeysekera

School of Engineering, Cardiff University, Wales, United Kingdom

HIGHLIGHTS

- A model to quantify the cooling demand of housing communities due to climate change.
- Provision to assess different active and passive cooling strategies.
- Location and orientation of houses in the community affect their cooling demand.
- Demand datasets to design cooling networks can be generated with the model.
- Open-sourcing the Modelica model to enable customisation for different communities.

ARTICLE INFO

Keywords:
Cooling demand
Housing community
House envelope
Modelica
Cooling load mitigation

ABSTRACT

Global warming has led to higher ambient temperatures in traditionally cold regions in Europe such as the UK. While implementing strategies in residential dwellings to meet the rising demand for cooling during hot summers is thus of interest, an accurate estimation of such demand is however a prerequisite for developing or implementing upgrades to cooling infrastructure. To contribute to this effort, this paper presents an estimation tool to quantify the cooling demand of a housing community. The tool was developed with the open-source software OpenModelica and was used to model diverse heat transfer phenomena in house envelope components, individual houses, and groups of houses. It uses multiple levels of design hierarchies and enables exploring different heat mitigation strategies. The tool was employed to estimate the potential future cooling demand of a UK housing community. The results highlight that houses of the same design may exhibit substantial variations in demand based on their location and orientation within the community. For instance, the annual demand of the houses ranges from 4505.8 kWh to 5873.4 kWh for the years under study if a cooling setpoint temperature of 21°C is adopted. By increasing this setpoint by 1.5°C, the community's annual demand could be reduced by ~20 MWh. Furthermore, incorporation of mitigation strategies reduced both the overall and peak demands for the individual houses and the community as a whole while also decreasing the disparity in demand across households. By having access to the estimation tool, shared alongside the paper, interested users may be boosted to conduct ad-hoc assessments to understand cooling demand variations within any housing community of interest.

1. Introduction

Climate change is already having significant global impacts, including increased occurrences of wildfires, prolonged droughts, and unusual intensities of wind and rain [1]. One notable consequence is the escalating frequency and intensity of heatwaves [2]. The United Kingdom (UK), once considered a cold country, is no longer exempt from the devastating effects of extreme heatwaves, with the risk of increased excess deaths due to extreme heat in the coming years [3]. In fact, the record-breaking heatwave experienced in July 2022 was considered a likely result of climate change [4]. Heatwaves in Europe have already caused nearly 90,000 fatalities since 1980 [5]. Even with temperature stabilisation at 1.5°C above pre-industrial levels by 2100, over 100 million Europeans annually will face heatwaves that are currently deemed intense [5].

Adverse climate effects are likely to continue unless net-zero emission targets are achieved throughout the globe—set for 2050 (at the latest) for the UK [6], EU [7] and the other signatories of the 27th UN Climate Change Conference. Several countries worldwide have already adopted decarbonisation strategies aimed at alleviating the detrimental impacts of climate change through the deployment of renewable energy

* Corresponding author.
E-mail address: Ugalde-LooC@cardiff.ac.uk (C.E. Ugalde-Loo).

https://doi.org/10.1016/j.apenergy.2024.124597
Received 11 July 2024; Received in revised form 24 September 2024; Accepted 25 September 2024

Nomenclature and variables

Abbreviation / variable definition

CIBSE	Chartered Institution of Building Services Engineers
RMSE	Root mean square error
UKCP	UK Climate Projections
1D	One-dimensional
c_p	Specific heat [J/(kg-K)]
h_i, h_o	Indoor and outdoor convective heat transfer coefficients [W/(m^2-K)]
k	Thermal conductivity [W/(m-K)]
t	Time [s]
v	Average wind speed [m/s]
A	Surface area [m^2]
I	Solar radiation incident on unit area of the envelope surface [W/m^2]
$Q_{c,in}$, $Q_{c,out}$	Convective heat transfer between the surfaces of building envelope and the indoor and outdoor air [W]
ΔR	Long wavelength radiation exchange between the envelope surface and ambient [W/m^2]
T	Temperature [K]
T_{in}	Indoor air temperature [K]
T_{int}, T_{ext}	Interior and exterior surface temperatures of building envelope [K]
T_{sol}	Sol-air temperature [K]
α	Solar absorptivity
ε	Long wavelength emissivity
ρ	Density [kg/m^3]
τ_i, τ_o	Transmissivities of inner and outer glass panes

technologies [8]. With expected warmer climate conditions in the future, there is a growing demand for cooling provision to maintain thermal comfort and prevent overheating [9]. As such, it is imperative for governing authorities to ensure this demand is met by adopting sustainable technologies and ideally passive strategies where a balance between comfort and environmental responsibility is achieved [10].

An important aspect of achieving decarbonised cooling involves quantifying the rising energy demand for space cooling in the face of evolving climatic conditions. Accurate estimations are necessary to understand the required changes in energy infrastructure and operations of cooling systems to meet the expected increased energy requirements [11]. These will also help determine key locations that need to be focused on to upgrade electricity distribution grids to support housing communities in the upcoming years. While several countries in Europe have well-established systems and networks for space heating (and even district cooling), limited progress has been made in the UK on space cooling systems as these have not been traditionally required and are emerging [12]. Consideration of cooling demand in the UK research and policy landscape is still lacking [13].

Building energy simulation tools play a vital role in quantifying the thermal requirements of buildings [14]. These tools are utilised to model and analyse diverse factors influencing energy consumption, including heating, cooling, lighting, and ventilation. Several software engines are available for this purpose, including EnergyPlus, IDA ICE, DesignBuilder, IES VE, Ansys, TRNSYS, and OpenModelica. These enable developing and executing numerical models that consider inputs such as weather conditions and building material properties to assess heat transfer and indoor temperature profiles within living spaces [15].

In the context of cooling buildings in warm ambient conditions, the aforementioned software tools have been widely utilised to model heat transfer in buildings and their various components. For instance, in [16] Ansys Fluent was employed to simulate heat transfer across a single building wall, while the same software was utilised in [17] to model indoor temperature and airflow profiles in a healthcare ward by considering different configurations for fresh air supply and retrofitting of the ward envelope. DesignBuilder and EnergyPlus were utilised in [18] to model and optimise the cooling performance of residential buildings situated in a hot semi-arid climate, while IDA ICE was employed in [19] to model and evaluate the effects of different street canyon geometries and orientations on the cooling load of a high-mass family apartment in a hot desert environment. In [20], IES VE was used to assess the thermal performance of a detached family house with a passive downdraught evaporative cooling tower in the hot climate of Saudi Arabia, while in [11,21,22], also using IES VE, the impact of building fabric, orientation, and geographical location was assessed for the most common building typologies in the UK (i.e. apartments, bungalows, detached houses, semi-detached houses, and terraced houses).

In [23], TRNSYS was used to model the cooling and heating demand of a residential house. The reference highlighted the importance of accurately estimating energy demand for indoor space conditioning, as this would dictate the types of thermal systems (and their capacities) to meet energy demand with the lowest cost of installation. Also using TRNSYS, [24] demonstrated the adoption of a heat pump-based energy system to meet both the heating and cooling demand of a residential building located in Cardiff, Wales. Weather data files for the specific location were adopted to assess system performance under different seasons and occupancy patterns. Arguably, such inferences and solutions would also apply to residential communities. At the same time, an accurate estimation of cooling demand across groups of households in a warming climate would be key to understand how much capacity expansion would be required in the electricity distribution grid infrastructure to cater for large cooling demand in the upcoming years. A tool which determines the cooling demand of residential communities would be useful for such task.

While studies have been conducted on modelling district cooling systems for housing communities using simulation software like Modelica [25] and TRNSYS [26], there are limited alternatives to determine the cooling demand input for such models. Although several models available in the literature (many of which were discussed in previous paragraphs) enable quantifying thermal demand in buildings and these models could be arguably aggregated to represent housing communities, most have been developed in proprietary platforms. To have wide usability of cooling demand quantification tools for houses and communities at different scales, availability of open-source platform-based model development is critical. There have been some developments in this regard. For example, Ref. [27] presents an open-source implementation in Modelica for a net-zero energy community. However, the energy demand in buildings was modelled by assuming historical patterns of usage of some appliances and assigning a constant load for other appliances which would normally have highly fluctuating loads. The model therefore did not accommodate detailed heat transfer dynamics through the building envelope. More importantly, the model is difficult to be adopted for energy demand quantification under future climate projections not conforming with the historical data.

While the Modelica programming platform has been extensively used for energy modelling of buildings and communities, a recent review on this aspect in [28] highlighted that the majority of these models were developed in the commercial development environment Dymola, which again limited the scope of open-usability of such models. The same reference recognised that the use of open-source libraries in open-source development environment (e.g. JModelica and OpenModelica) would be a hotspot for further progress with pure open-research in this domain. In addition, the development of building energy models in Modelica has been prominent in United States, Germany, Belgium, and

France [28], but limited case studies for the UK exist.

On the other hand, the popular open-source programming language Python has also been used for energy modelling of buildings and communities [29,30]. However, such models do not offer a convenient graphical user interface (GUI) for building modelling. Therefore, it becomes essential for building energy modellers to be experienced in computer programming if a complex model is to be developed when adopting this modelling approach. Besides, such intricate computer codes would naturally attract a smaller end-user base compared to software packages offering modelling and interpretation through both programming and graphical interfaces.

From the previous discussion, the absence of an open-source tool to quantify cooling demand of buildings and communities with the flexibility of both enabling programming and providing graphical interface-based energy modelling represents a gap in the research domain. While OpenModelica offers these capabilities, there has been limited development of such models in this environment, and even more limited developments assessing cooling demand of UK's residential communities, which is now becoming an emerging issue. To bridge this gap, this paper makes the following contributions:

1. A community-level cooling demand estimation tool developed using Modelica is presented. The tool models the transient heat transfer through the envelopes of a group of houses. It is based on a model that considers the weather parameters in the community premises and quantifies the cooling demand of individual houses and the entire community. It accounts for shading effects of neighbouring houses and wall-sharing between attached houses to account for the spatial characteristics of the community. The model has provisions to design different construction assemblies and dimensions, blind control schemes, and cooling system operation settings.
2. Cooling demand profiles for a UK-based residential housing community determined with the estimation tool are provided. Using temperature projections obtained from UK Climate Projections (UKCP) issued by the Meteorological Office [31], the aggregated and individual cooling demand profiles were generated. This enabled studying the effects of location and orientation of houses within the community and the consequent impact on cooling demand.
3. The tool for community-level cooling demand estimation has been open-sourced and made available with this paper. This will enable users to develop custom models of different houses and communities and assess their cooling demands under different climatic conditions. The free access to the tool is envisaged to support modelling and simulation of cooling networks and technologies in different platforms requiring cooling demand data as an input.

2. Material and methods

2.1. Details of the housing community

The housing community comprises 31 similar houses situated in a town in the UK at an approximate latitude of 50° North. Each house has a different location and orientation within the community. For the purpose of data privacy, the longitude and actual name of the community have been anonymised.

Fig. 1 provides an aerial view of the community and a schematic representation of the individual houses. Numbered walls and roof sections that constitute the respective envelopes of the houses are included for clarity. Fig. 2 shows allocated house numbers within the community. Table 1 lists the areas of the walls and roofs. The internal volume of each house within the community is 499.9725 m^3.

2.2. Weather data

The primary weather factors influencing the thermal energy demand of houses are solar radiation and ambient temperature. The solar

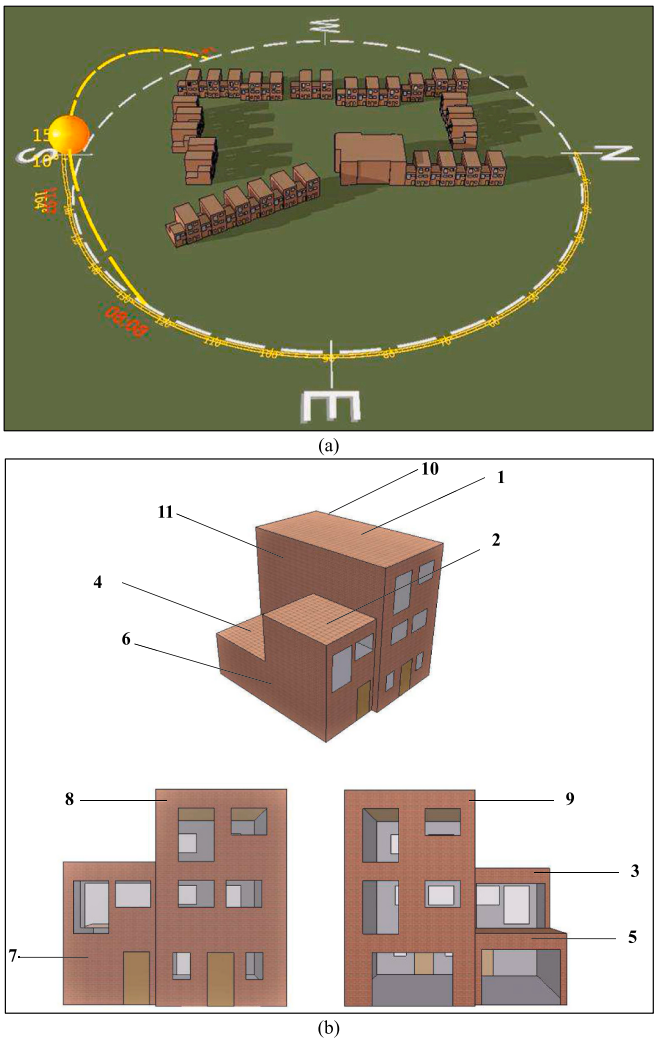

Fig. 1. (a) Aerial view of the community. (b) Schematic of the houses with wall and roof numbering.

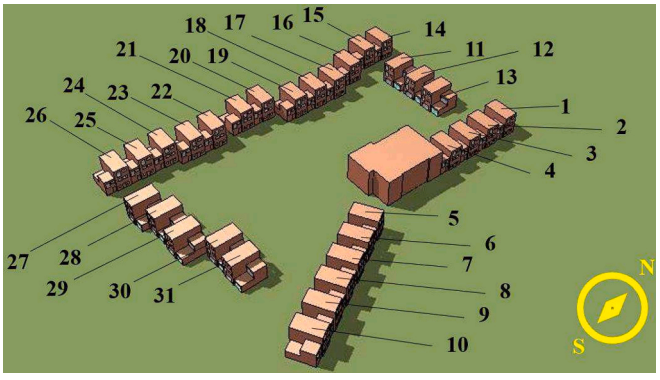

Fig. 2. House numbering within the community.

radiation data required for the analysis was obtained from weather files published by the Chartered Institution of Building Services Engineers (CIBSE) [32]. These files provide inputs such as direct and diffuse radiation values, solar altitude, and azimuth angles, which are crucial for calculating the incident solar radiation on external surfaces of buildings.

IES VE was adopted to model solar radiation and to ensure reliability and accuracy of the obtained results, as this software has been validated in the past against internationally recognised standards such as ASHRAE

Table 1
Areas of walls, roof, and floor of an individual house.

Wall / Roof no.:	1	2	3	4	5	6	7	8	9	10	11	Floor
Total area [m^2]	46.28	15.44	9.59	15.44	9.59	35.24	19.17	40.1	40.1	75.74	40.5	77.16
Window area [m^2]	0	0	6.3	0	6.38	0	4.05	8.05	14.2	0	0	0
Door area [m^2]	0	0	0	0	0	0	2	2	0	0	0	0

140, CIBSE TM33, and ISO 52000 [33]. The Hay model [34] was used to this end, which has been integrated to IES VE as a built-in simulation tool. The software provides a high-level GUI to create 3-dimensional (3D) prototypes of houses of any desired shape and allows the information of the latitude of the house location to be fed into the model [35]. Using the information of the geometries and orientation of houses and their location, the Hay model is used to obtain the incident radiation on each wall and roof of the houses on an hourly basis [34].

IES VE offers an automated process for integrating building shapes into the simulation environment [35]. Upon importing or creating a 3D house model in the GUI, the software automatically generates the necessary geometric parameters, including surfaces, orientations, and shading elements, which are then used by the Hay model to calculate solar radiation on different parts of the house.

Through the utilisation of 3D modelling, IES VE enables the consideration of adjacent buildings and structures. This allows for an accurate assessment of shading effects on the building surfaces. This approach offers a significant improvement compared to standard methods where shading effects are approximated using constants applied uniformly to the model, with variations based on the degree of shading (low, medium, or high) [34]. The use of IES VE thus allows for a higher level of precision in the modelling of incident solar radiation on different house facades.

IES VE also allows for the inclusion of additional shading elements like roof overlaps, nearby buildings, and trees. These elements are modelled within the software by either importing them as part of the 3D geometry or by manually adding them using the software's built-in tools [35,36]. The Hay model then accounts for the shading effects of these elements in its calculations. In fact, in the verification exercise of the house model in Modelica reported in Section 2.4.2 of the paper, the shading effects of neighbouring trees and houses on the real house investigated in [37] were modelled in IES VE and the consequent radiation data was used as input to the Modelica model of the experimental house.

As a way of an example, the incident radiations on 3 different walls and 1 roof belonging to 4 different houses within the community under study shown in Fig. 2 are presented in Fig. 3.

Data was sourced from the UKCP database to obtain the ambient temperatures for the housing community. This database offers spatially mapped ambient temperature projections for future years provided at hourly values. For this paper, temperature projections until 2040 were accessed. From the retrieved data, two different years were selected for further analysis. Firstly, year 2025 was chosen due to the high number of instances where the projected ambient temperature surpassed a threshold of 24°C as this could be deemed uncomfortable [38]. Secondly, year 2035 was selected as it aligns with the UK Government's target year for decarbonising its electricity sector [39]. The ambient temperature profiles for the selected years are presented in Fig. 4.

2.3. Model development in Modelica

The community-level cooling demand estimator was modelled using

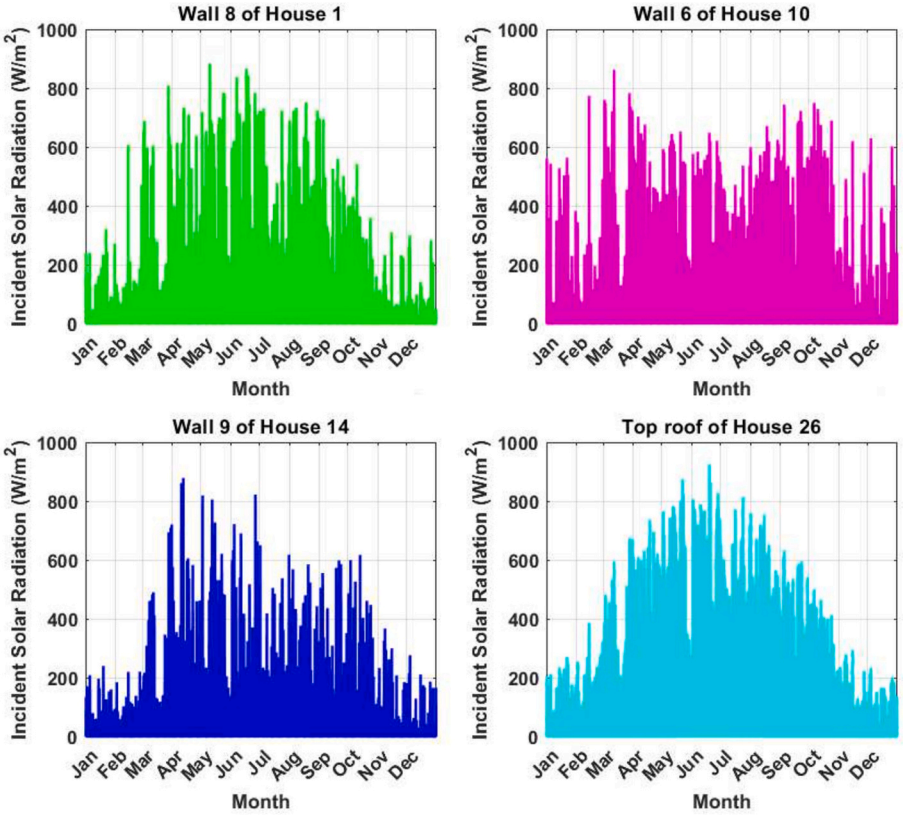

Fig. 3. Incident solar radiation on different walls and roof of 4 different houses in the community.

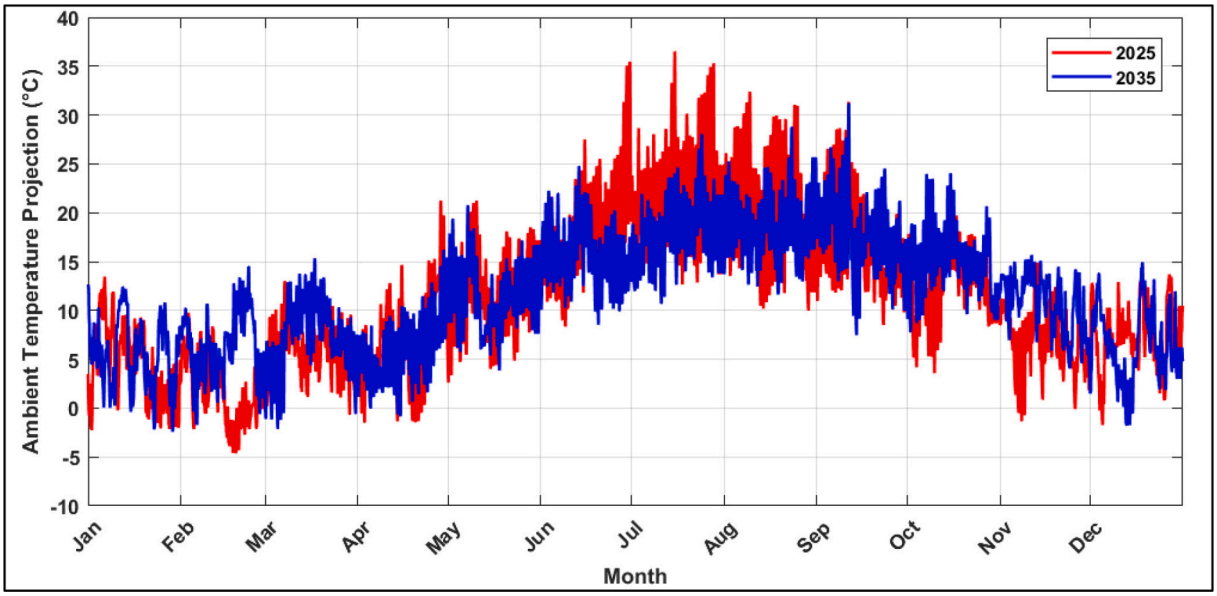

Fig. 4. Ambient temperature projections from the UKCP database for years 2025 and 2035.

Modelica with OpenModelica as the design and development platform. The development followed a bottom-up approach involving three levels of modelling hierarchy as described next.

2.3.1. Level 1: modelling house envelope components

This is the fundamental modelling level that underpins the physics of heat transfer across the structural components of the house envelope such as walls, roofs, windows, and doors. Principles of one-dimensional (1D) transient heat conduction through multiple material layers were employed to quantify the inward and outward heat transfer through the envelope components. For this purpose, the "Multilayer" block of conduction heat transfer from Modelica Buildings Library was used [40]. For different envelope components, adequate dimensions and thermophysical properties were assigned through this block for all material layers. This information is provided in Table 2.

Table 2
Thermophysical properties and thicknesses of structural layers in different envelope components [42,43].

	Material	Thickness [mm]	Thermal conductivity [W/(m-K)]	Density [kg/m^3]	Specific heat [J/(kg-K)]
Wall	Rainscreen	3	50	7800	450
	Cavity	50	0.026	1.225	1000
	Insulation	81.4	0.025	20	1030
	Cement bonded particle board	12	0.23	1100	1000
	Cavity	50	0.026	1.225	1000
	Plasterboard	12.5	0.21	700	1000
Roof	Insulation	154.4	0.03	40	1450
	Membrane	0.1	1	1100	1000
	Concrete deck	100	2	2400	1000
	Cavity	50	0.026	1.225	1000
	Plasterboard	12.5	0.21	700	1000
Window	Outer glass	6	1.06	2500	800
	Cavity (Argon)	12	0.01772	1.633	520.3
	Inner glass	6	1.06	2500	800
Door	Wood	44	0.14	650	1200

To calculate the 1D transient heat transfer through each material layer, Modelica solves the diffusion Eq. [40].

$$k\frac{d^2T}{dx^2} = \rho c_p \frac{dT}{dt} \tag{1}$$

where k is the thermal conductivity [W/(m-K)], T is the temperature [K], x is the thickness [m], ρ is the density [kg/m^3], c_p is the specific heat [J/(kg-K)], and t is time [s].

Convective heat transfer between the surfaces of the building envelope and the indoor and outdoor air, $Q_{c,in}$ and $Q_{c,out}$ [W], are modelled using

$$Q_{c,in} = h_i A(T_{int} - T_{in}) \tag{2}$$

$$Q_{c,out} = h_o A(T_{sol} - T_{ext}) \tag{3}$$

where A [m^2] is the surface area of the envelope component, T_{int} [K] is the interior surface temperature of the envelope, and T_{ext} [K] is the exterior surface temperature of the envelope. T_{in} [K] is the indoor air temperature, and T_{sol} [K] is the sol-air temperature that combines the effects of solar radiation and heat convection of the envelope with the outdoor ambient [41]. In (2), h_i [W/(m^2-K)] is the indoor convective heat transfer coefficient, while h_o [W/(m^2-K)] in (3) is the outdoor heat transfer coefficient. T_{sol} is calculated with [17]

$$T_{sol} = T_o + \frac{\alpha I}{h_o} \quad \text{(for a wall)} \tag{4}$$

$$T_{sol} = T_o + \frac{\alpha I}{h_o} - \frac{\varepsilon \Delta R}{h_o} \quad \text{(for the roof)} \tag{5}$$

where α is the solar absorptivity and ε is the long wavelength emissivity of the outer surface of the building envelope, with assigned values $\alpha = 0.75$ and $\varepsilon = 0.9$ [44,45]. Also in (4) and (5), I [W/m^2] is the solar radiation incident on unit area of the envelope surface and ΔR [W/m^2] is the long wavelength radiation exchange between the envelope surface and ambient, which was assigned a value of $\Delta R = 63$ W/m^2 [46]. In addition, it was assumed that $h_i = 5$ W/(m^2-K) [47], whereas h_o was calculated with the McAdams model [48,49] as

$$h_o = 5.678\left[0.99 + 0.21\left(\frac{v}{0.3048}\right)\right] \tag{6}$$

where v is the average wind speed. For an average wind speed in the UK of $v = 4.48$ m/s [50], using (6) leads to $h_o = 23.15$ W/(m^2-K).

Fig. 5 shows a screenshot of the wall model implemented in Modelica. It receives as input the incident solar radiation, outdoor ambient temperature, and cross-sectional area of the wall. The output is the net heat flow rate through the wall. To be able to represent different walls within a house with different cross-sectional areas A, a value of $A = 1$ m^2 was hard-assigned in the multilayer conduction block to calculate the heat flux q' [W/m^2]. This value was then added to the factor $(A-1)q'$ to obtain $q'A$ [W], which is the net heat flow rate through a wall with cross-sectional area A assigned through an input link.

The window model, shown in Fig. 6, introduced a slight variation to the wall model just described by incorporating radiative heat gain in addition to the conductive heat transfer through the window. The radiative gain was calculated by multiplying the incident solar radiation with the transmissivities of the outer and inner glass panes, with values $\tau_o = 0.409$ and $\tau_i = 0.783$ [42,43].

Shading on windows due to other houses was modelled by adjusting the solar radiation input. For instance, if a neighbour house casts a shadow on the window of a particular house, the radiation input would be adjusted by the Hay model in IES VE by accounting for the shadows. The consequent solar radiation was used as input to the Modelica model for the window.

The window model also included a module for internal blind operation. This allowed for the blinds to be partially closed (using a percentage) when the indoor temperature had surpassed a predefined threshold value. This operation scheme was intuitively determined and was assumed as subjected to occupants' preferences. As such, the model allows for adjusting the blind opening percentage and the setpoint temperature for blind controls, giving users the flexibility to tailor these parameters as required. The effects of these settings on the cooling demand are discussed later in Section 3.2.

The models for roofs and doors resemble the wall model in terms of fundamental heat conduction modelling. The interested readers are referred to Appendix A for further details.

2.3.2. Level 2: modelling individual houses

This is the second level in the modelling hierarchy, where the heat gain and loss for an individual house is computed by aggregating the heat transfer through all envelope components of the house. Additionally, a model for heat transfer through the floor was implemented at this level. A multilayer conduction block was used for this considering the material dimensions and properties for each layer defined in Table 3. A ground temperature of 12.7°C was considered given the selected location in the UK [51].

The floor model was instantiated in Level 2 rather than in Level 1 because only one instance of the model was used for an entire house, unlike the other envelope components that had multiple instances in one house, and therefore benefitted from the general template created in Level 1.

Internal heat gains were also modelled within Level 2 using ISO-recommended profiles for occupants, appliances, and lighting in residential houses per unit floor area [52]. These profiles were scaled for the individual houses by multiplying the heat gains with the floor area (77.16 m^2).

Different profiles for internal heat gains were used for weekdays and the weekend, as provided in [52]. The total internal heat gain was obtained by aggregating the contributions from all sources. This was then applied as a heat source to the house model with a periodicity of 7 days. Fig. 7 shows the weekly-periodic profile from Monday to Sunday. Given that the first day of year 2025 is Wednesday and that of 2035 is Monday, the profiles were adjusted to start on the respective day of the week. For simplicity, changes in internal heat gains due to holidays and seasonal variations were not considered.

The following rationale was considered to quantify the cooling demand of a given house. If the indoor temperature were to rise above the cooling setpoint temperature, the house would be cooled by introducing cold air at a predefined supply temperature. The flow rate of such supply air would vary between predefined maximum and minimum values. The energy required to cool the outside ambient air to the indoor supply temperature would be considered as the cooling demand. This value was calculated within the house model by implementing a sensible cooler block [53].

Heating of the house during cold conditions was done by implementing a radiative heater [53]. However, for clarity, heating is not discussed in this paper. A screenshot of the cooling circuit along with the building envelope components in the house model implemented in Modelica are shown in Fig. 8. An equivalent block diagram is presented in Fig. 9 to enable an easier interpretation of the house model. A detailed explanation of the different component assemblies in the house model is

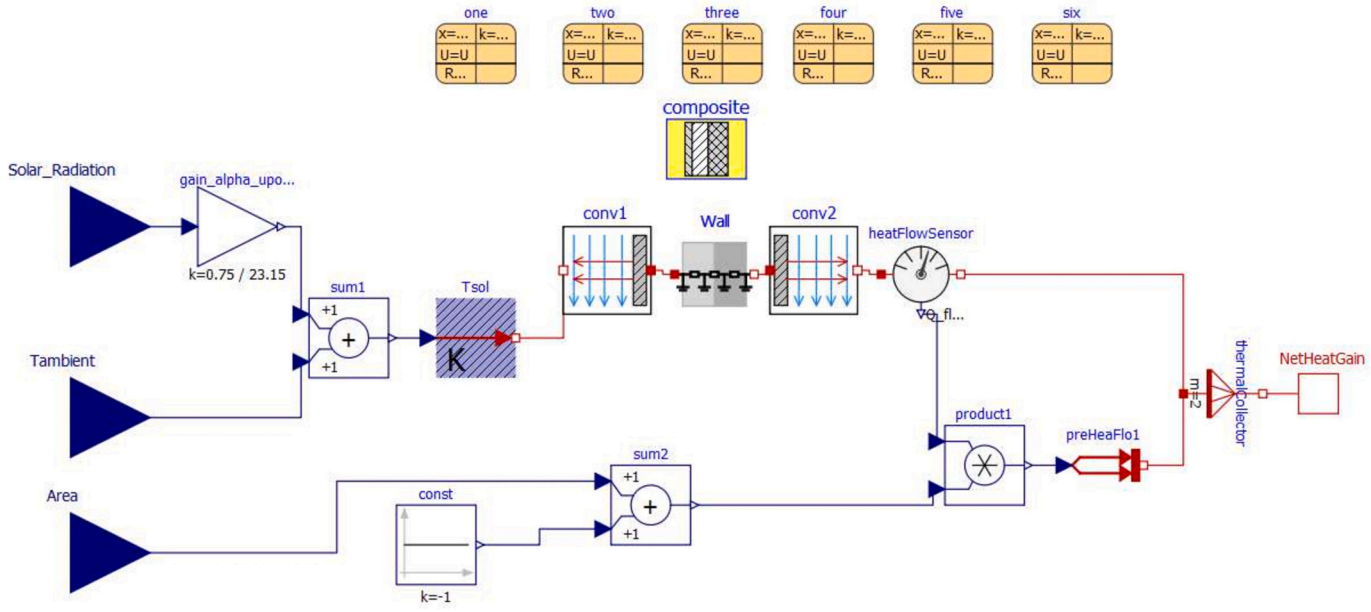

Fig. 5. Screenshot of the wall model implementation in Modelica.

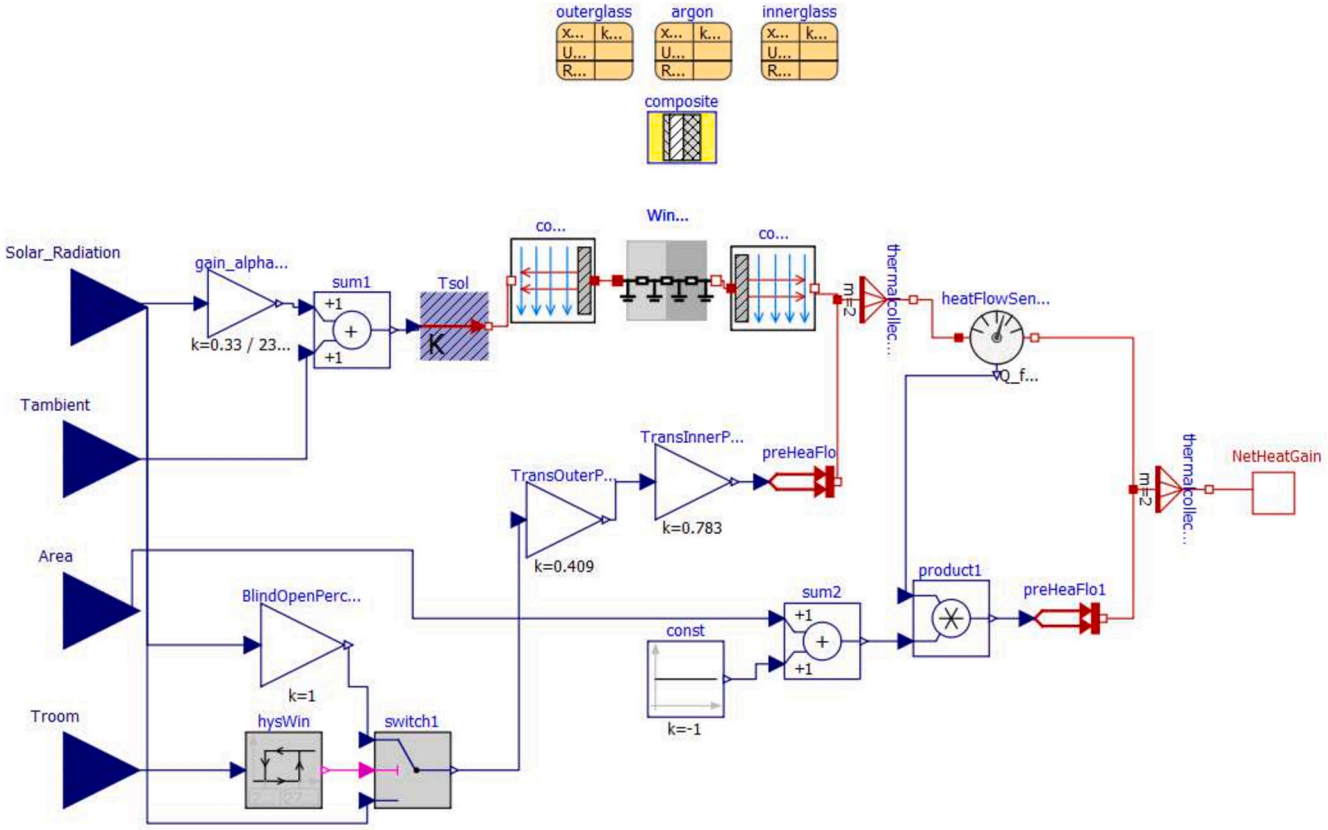

Fig. 6. Screenshot of the window model implementation in Modelica.

Table 3
Thermophysical properties and thicknesses of structural layers in floor model [42,43].

Material	Thickness [mm]	Thermal conductivity [W/(m-K)]	Density [kg/m^3]	Specific heat [J/(kg-K)]
Insulation	98.2	0.025	700	1000
Reinforced concrete	100	2.3	2300	1000
Cavity	50	0.026	1.225	1000
Chipboard flooring	20	0.13	500	1600

provided as supplementary material along with this paper.

2.3.3. Level 3: modelling the community

The output values of cooling demand obtained from the individual houses in Level 2 were aggregated at this level to obtain the cooling demand for the entire community. "Radiation" and "AmbientTemp" components were utilised to read input data on solar radiation and ambient temperature from external source files. These readings were then consolidated in the "weatherBus" component, which subsequently delivered the radiation data as input signals to the respective houses. As for the ambient temperature, since it remained consistent across all houses, it was directly supplied from "AmbientTemp" to the respective houses.

Note: Currently, there is no direct interface between IES VE and OpenModelica for solar radiation and shading information exchange. For the case studies presented in this paper, solar radiation data from IES VE was exported as a CSV file, which was read by the "Radiation" block.

Additionally, the "InternalHeatGainProfiles" component read an external file with the weekly periodic profile shown in Fig. 7 with hourwise values of internal heat gain from occupants, appliances, and lighting. These data were then processed by the house models at Level 2.

The components used in the models have dependencies on the Modelica Standard Library (Version 3.2.3) [54] and Buildings Library (Version 8.10) [55]. An artificial time period of 1 h was added at the beginning of all simulations to eliminate any inconsistencies during model initialisation. Further information about the simulation setup is available along with the Modelica models in the supplementary material accompanying this paper.

2.4. Model verification

Based on the experimental data available in existing literature, the models developed in the previous sections were verified at envelope component level and individual house level.

2.4.1. Verification at envelope component level

The model for transient 1D heat transfer through multiple layers of envelope components (i.e. walls, windows, roofs, and doors) implemented in Modelica was verified by comparing the heat flux and temperature profiles obtained with the experimental results reported in [56]. In the reference, an experimental setup consisting of a closed cubicle with an interior periodic heat generation source was monitored for surface temperature and heat flux profiles over time. The material dimensions, properties of the cubicle walls, and the external surface temperature profiles were used as input data and boundary conditions for simulation with the model reported in this paper.

The model was simulated with Modelica's 'cvode' solver [57] with a time-step size of 45 s. Fig. 10 shows the comparison between the results obtained with the model and the experimental data. Although in [56] the indoor temperature was mentioned to be maintained at approximately 22–24°C, measured temperature values decreased to about 21°C at certain intervals. This would only be possible when the indoor

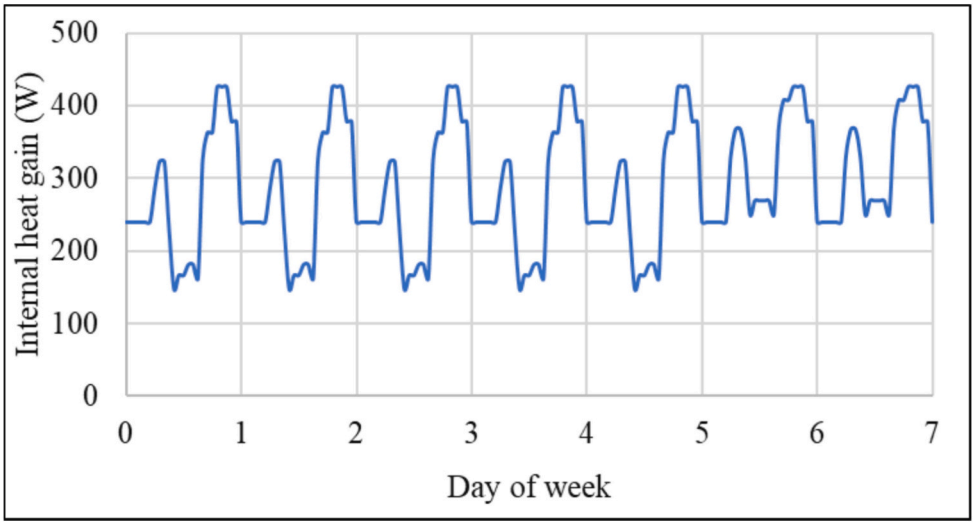

Fig. 7. Weekly periodic profile for internal heat gain in houses (Monday to Sunday).

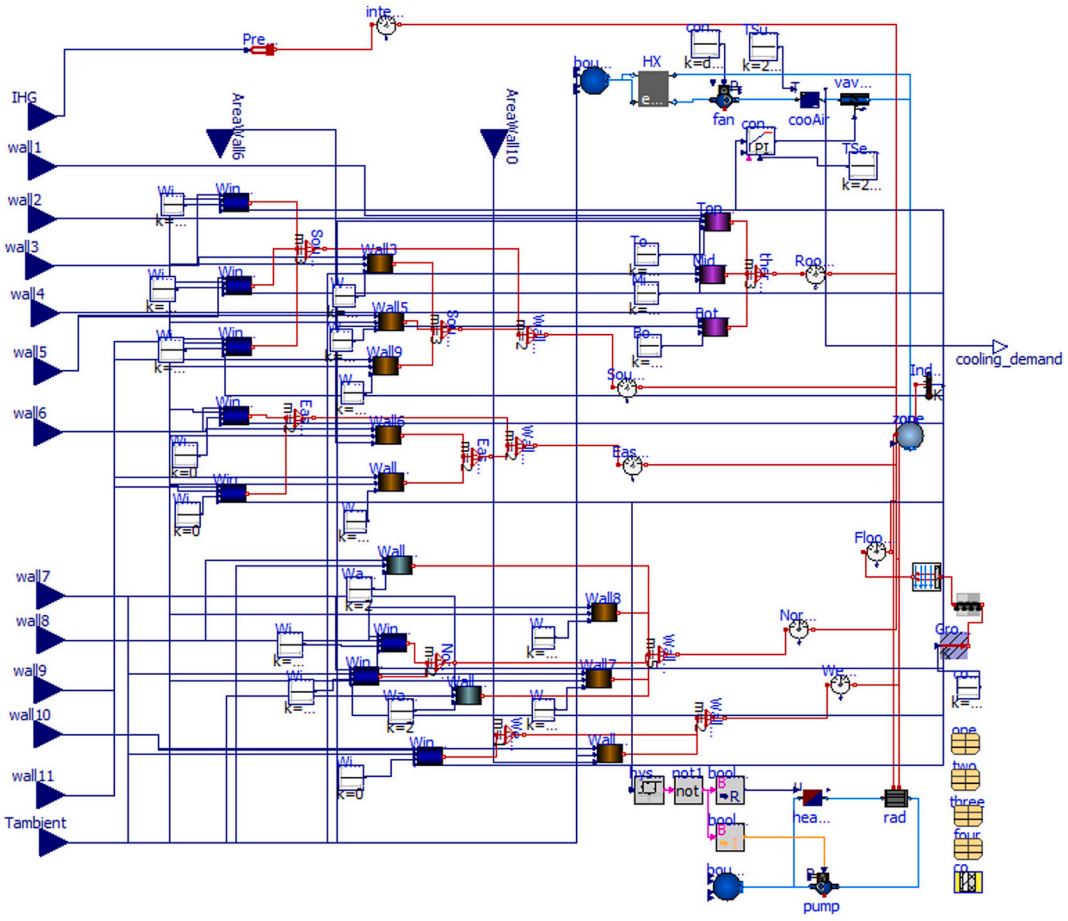

Fig. 8. Screenshot of the house model in Modelica.

temperature had dropped below 22°C to cool the surface to about 21°C as the external environment-facing surface of the cubicle was always above 22°C (see Fig. 10(b)). Taking into account these observations from [56], the indoor temperature was assumed to be 21°C for the model verification.

In general, a good agreement was achieved between both sets of results for heat flux and temperature variation, with a root mean square error (RMSE) of 0.67 W/m^2 for heat flux and 0.31°C for temperature. Therefore, the solver settings used in this verification exercise were adopted for the simulations presented later in the paper.

2.4.2. *Verification at individual house level*

An additional verification exercise was carried out to ascertain that the house model implemented in Modelica provided reliable results. For this, experimental results reported in [37] were considered. The experimental testing in the reference involved periodic monitoring of

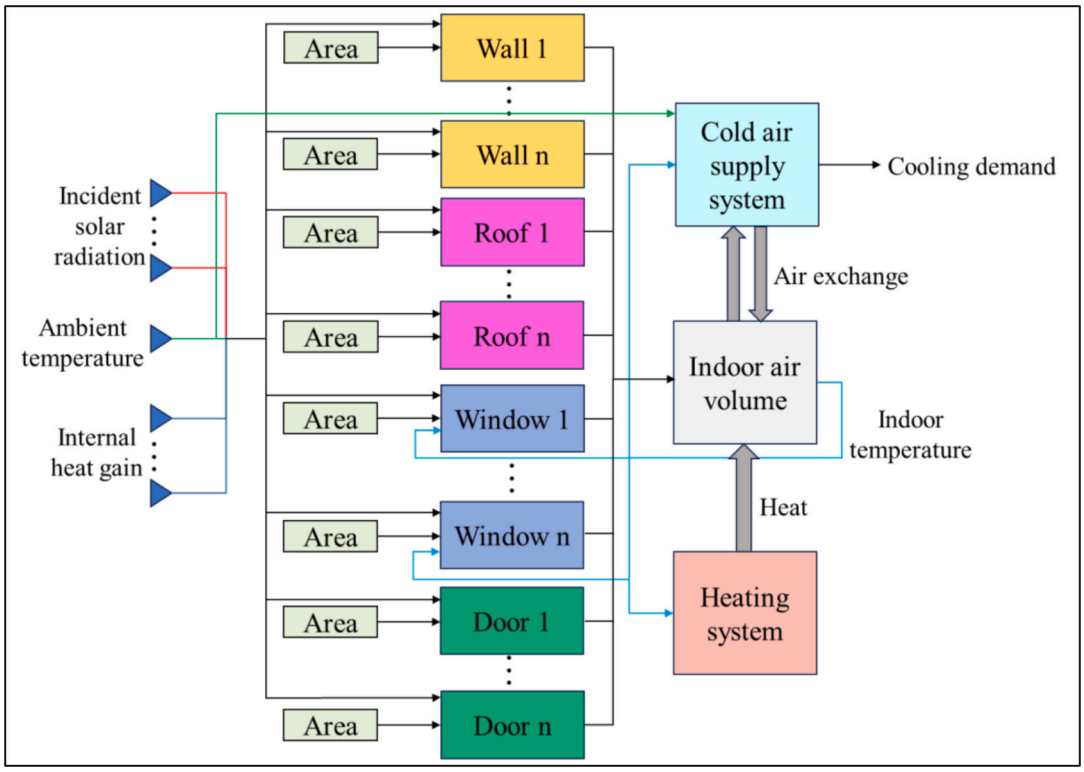

Fig. 9. Generalised block diagram of the house model for easier interpretation.

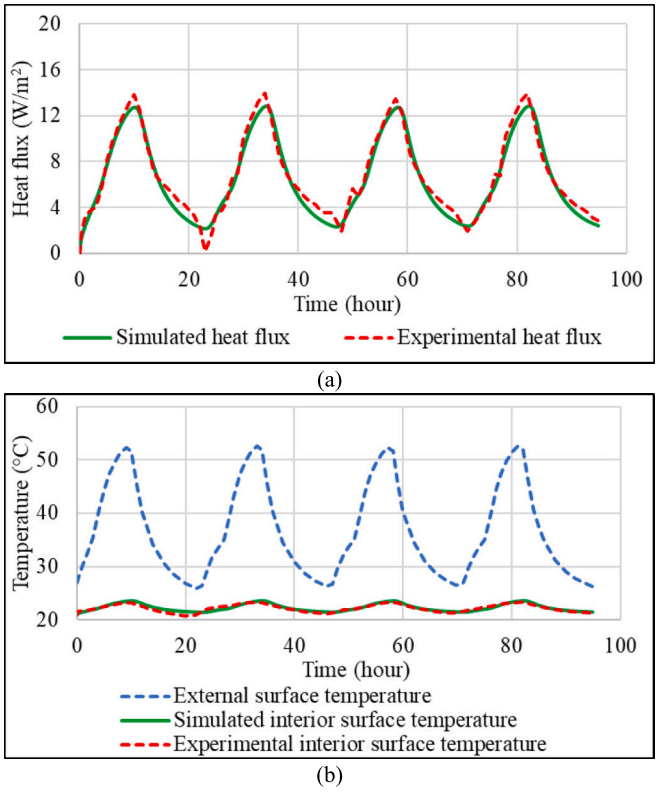

Fig. 10. Model verification with experimental results: (a) heat flux, (b) surface temperature.

the indoor and outdoor temperature of a full-scale semi-detached house located in Loughborough, UK, shown in Fig. 11.

Details of the construction materials and dimensions of the house were taken from [37] to prepare the equivalent model in Modelica. A screenshot of the software implementation is shown in Fig. 12. This model had a similar generalised block-level representation as shown in Fig. 9. The only difference was that the heating system block was absent as this effect was not assessed in the experiment. Also, the cold air supply system was adapted to inject air at ambient temperature with a fixed rate of 0.22 air changes per hour (ACH) as prescribed in the experiment. The measured hourly outdoor temperature for 4 months (June to September 2021) was used as the ambient temperature boundary condition for the equivalent model in Modelica. As for solar radiation, the measured values for incident radiation on different walls and roof of the actual house were not available. Therefore, these values were obtained using IES VE.

For simplicity, the house model assumed the entire indoor volume as a whole without any room partitioning. In the experiment, the hourly indoor temperature was monitored within each room of the house. As the numerical model outputs a single temperature value for the entire indoor air volume, the measured values for different rooms were weighted based on the individual room volume and averaged to enable a direct comparison between simulated and measured values. The model was then simulated for the period of 4 months (June–September) for which the measured data from the experiment was available.

The outputs of the model implemented in Modelica (blue trace) agreed with the experimental measurements (red trace) with a reasonable accuracy, as shown in Fig. 13, yielding an RMSE of 1.56°C. The difference in the results could be attributed to the approximation of the measured radiation quantities on each wall with the numerically computed values from IES VE. This could have led to differences in the rate of heat transfer from the external environment into the house, which in turn could have mildly influenced the indoor temperature. However, considering the data availability limitations and model simplification assumptions, the model showed good agreement with the

Fig. 11. Front view (a) and rear view (b) of the matched-pair houses used in the experiments in [37]. The house on the left in (a) was used for verification of the house model presented in this paper.

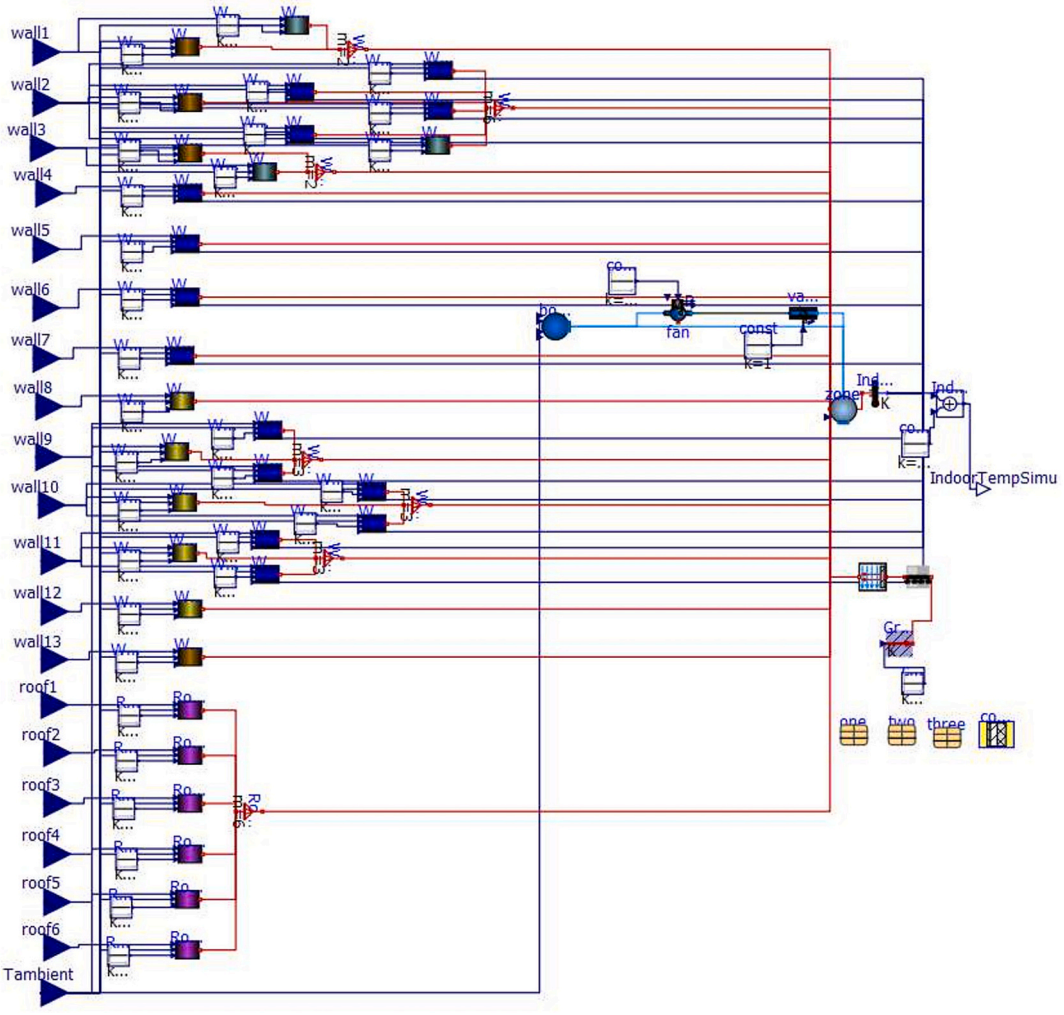

Fig. 12. Screenshot of the model implemented in Modelica equivalent to the experimental house in [37].

experimental results reported in [37].

3. Results and discussion

3.1. Cooling demand profiles and effects of house location and orientation

The community model was simulated to obtain cooling demand data for various houses and the aggregated cooling demand of the entire

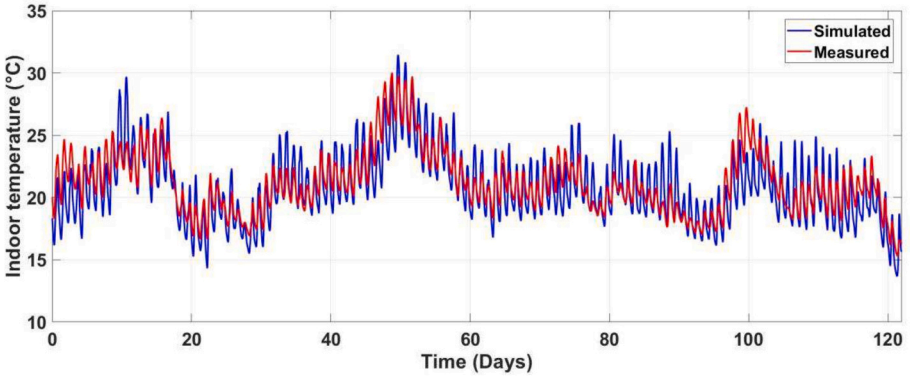

Fig. 13. Verification of the house model implemented in Modelica with experimental measurements in [37].

community. For clarity in the interpretation of results, Fig. 2 in Section 2.1 shows allocated house numbers within the community.

A base case for simulation was defined by considering specific settings in the houses. The cooling setpoint temperature was taken as 21°C [58] and the supply air temperature as 10°C for all dwellings. The supply airflow rate was controlled between a maximum of 4 ACH and a minimum of 0.2 ACH. The window blinds were assumed to be completely open.

Figs. 14 and 15 show the annual cooling demand profiles for five selected houses and the community as a whole for the years 2025 and 2035. Out of these five houses, four were located at the corners of the community, as observed in Fig. 2. The remaining house was selected as it exhibited the minimum cooling demand. The cooling demand profiles of all houses are presented in Appendix B.

There was a range of cooling demands among the houses, which could be attributed to differences in incident solar radiation on walls, roofs, and windows. These variations depended on the house location within the community, its orientation, exposure to solar radiation, and shading from neighbouring houses. These factors resulted in distinct cooling demand profiles.

To better visualise the differences in cooling demand among individual houses, the net annual cooling energy demand was calculated by integrating with respect to time the cooling power demand profiles shown in Figs. 14 and 15. These annual cooling energy demands were then processed into heat maps using IES VE. Figs. 16(a) and 16(b) display these heat maps for the years 2025 and 2035.

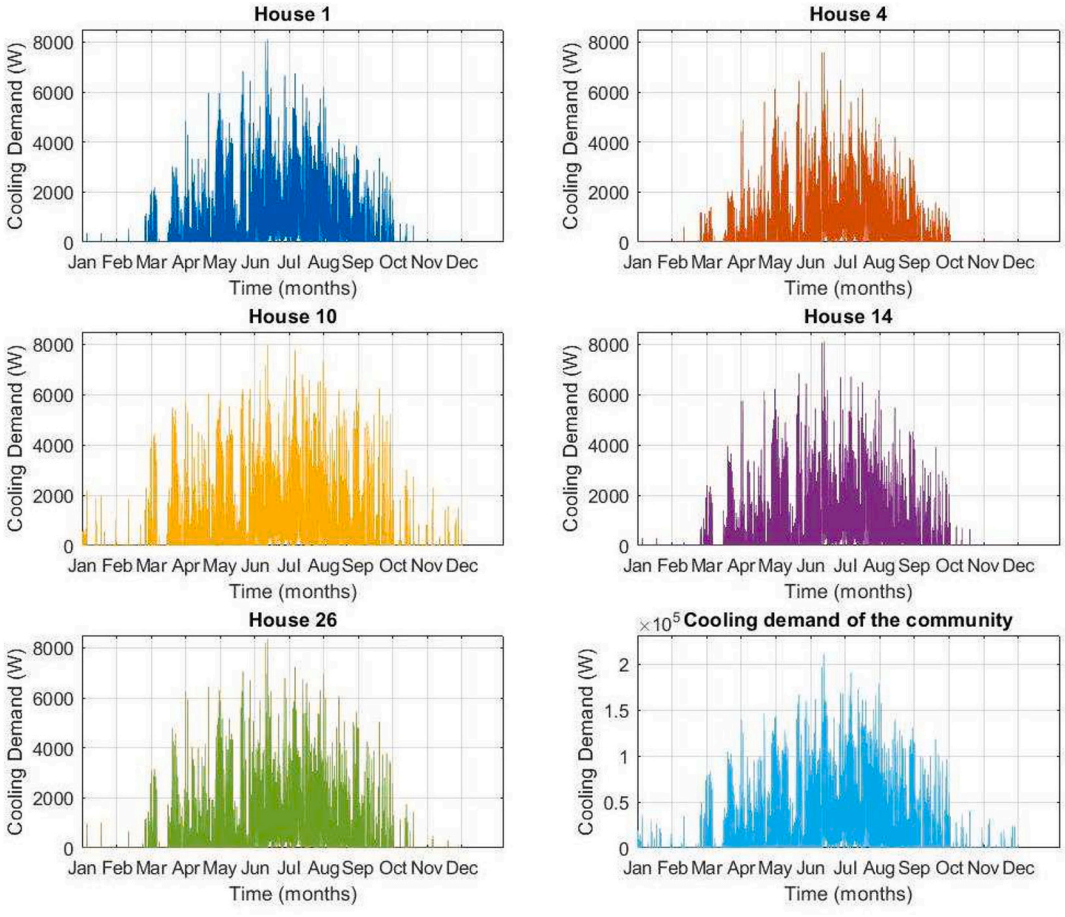

Fig. 14. Cooling demand profiles for different houses and the community for the year 2025.

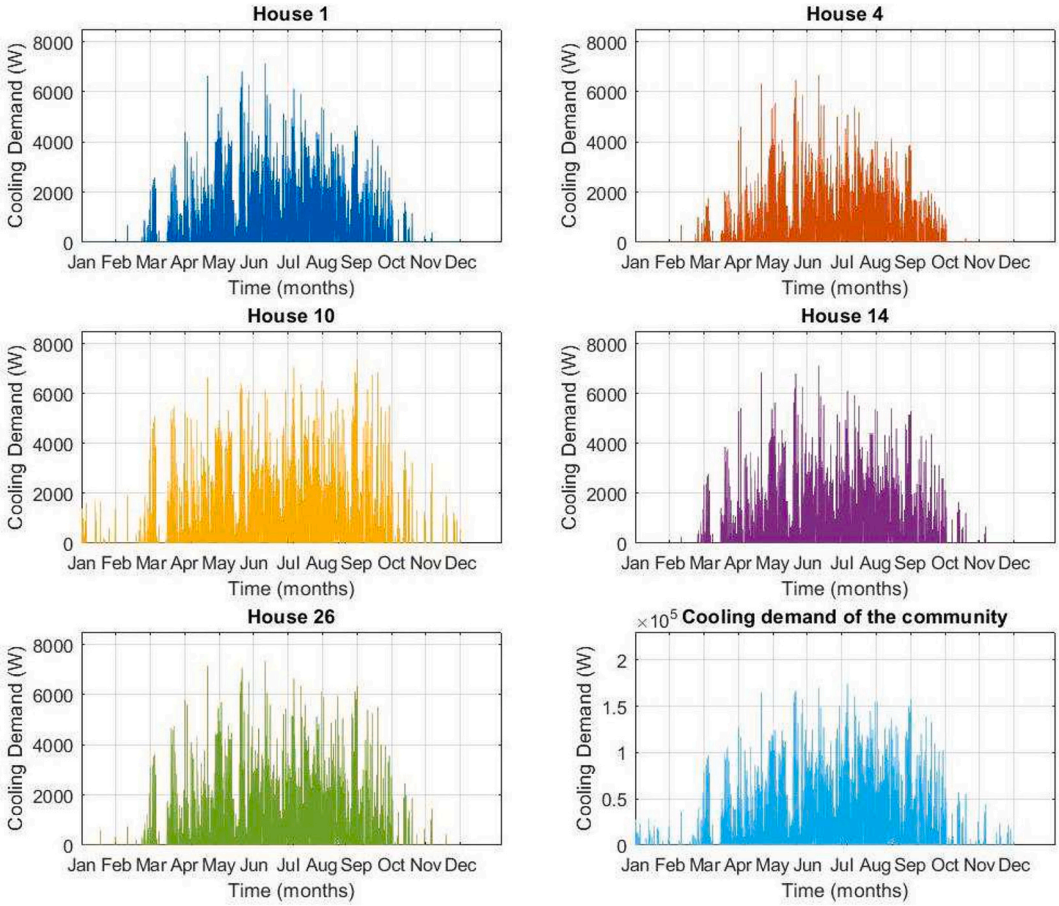

Fig. 15. Cooling demand profiles for different houses and the community for the year 2035.

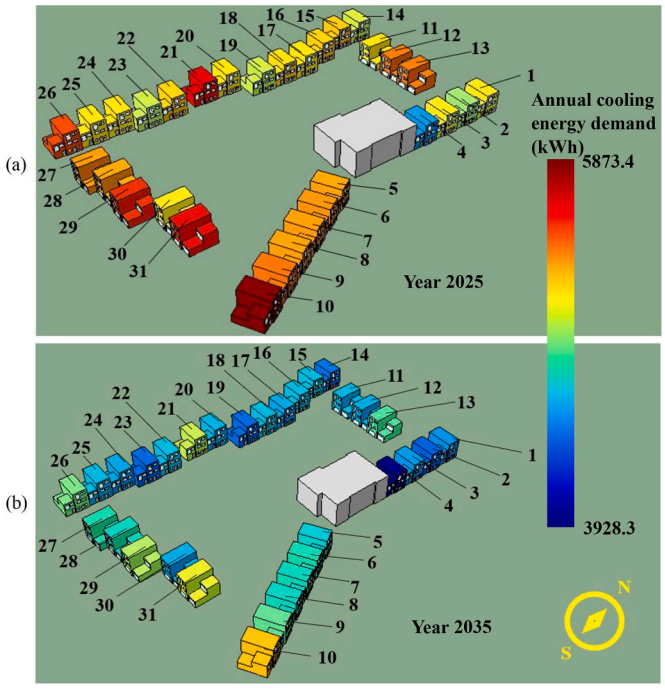

Fig. 16. Annual cooling demand of different houses in the community: (a) heat map for year 2025, (b) heat map for year 2035.

House 10 exhibited wider cooling demand profiles than the other houses. This is primarily due to its location in a sun-exposed corner of the community with minimal shading (see Fig. 2). The high intake of solar radiation through the windows with fully open blinds and no shading effect from neighbouring houses led to momentary cooling needs in the winter season. This unusual demand could be easily reduced through cooling load mitigation strategies (discussed later in Section 3.2 and Appendix C). On the other hand, House 14, positioned in the opposite corner, experienced significantly lower cooling demand, as depicted by smaller cooling peaks and a shorter annual time span for cooling demand, as shown in Figs. 14 and 15. This is also reflected through warmer colours of House 10 compared to House 14 in the heat maps shown in Figs. 16(a) and 16(b).

House 1, similar in orientation to House 14, displayed comparable cooling demand patterns. The consistent movement of the sun from east to west due south resulted in shadows cast from south to north throughout the day. This effect provided good shading for Houses 1 and 14. Therefore, these corner houses experienced a lower cooling demand compared to the other corner Houses 10 and 26. House 26 experienced a slightly lower cooling demand than House 10 even when they are located in the same southern corner (see Fig. 2). This could be attributed to minor differences in orientation and a shading effect from House 27 on the east side walls of House 26 during the late morning hours. House 10 received little such benefit from House 31 due to the skewed alignment and increased distance between the houses.

House 4 experienced minimum annual cooling energy demand in both years under investigation, as observed in Figs. 16(a) and 16(b). The cooling peaks and annual cooling demand span were also smaller for this house compared to the other houses (see Figs. 14 and 15). The reduced cooling demand was due to the shading effect of the large hall situated

on the south side of this house (unnumbered structure in Fig. 2).

House 18 had neighbouring houses on both the north and south sides. However, the presence of a neighbouring house on the north side did not provide shading benefits, leading to slightly higher cooling demand compared to corner Houses 1 and 14 (see Fig. 16). This was because House 18 lacked shading on its west or east-facing walls as no nearby houses were located in those directions. On the other hand, Houses 1 and 14 benefit from Houses 11, 12, and 13, which cast shadows on the northern corner houses during specific hours of the day.

House 19, despite being the south-side neighbour of House 18, exhibited a lower demand. This was due to the slightly staggered alignment of House 20 relative to House 19, resulting in enhanced shading effects on the rear walls and windows of House 19 in the afternoon hours.

The groups of south-facing houses (Houses 11–13) and (Houses 27–31) exhibited higher cooling demand compared to most of the other houses in the community. This was due to their different orientation and placement. Although they benefitted from shading either in the morning or in the afternoon hours from the houses located to their east or west, they received consistent solar radiation on the south-facing windows throughout the day. The increased radiation intake through the south-facing windows in these houses negated the effects of shading received from the east-facing house rows and led to an increased cooling demand. This is evidenced with warmer shades of the south-facing houses in Figs. 16(a) and 16(b).

Both individual houses and the community exhibited higher cooling demand in 2025 compared to 2035 (Figs. 14 and 15). This disparity is attributed to the variations in annual ambient temperature between the two years, with year 2025 anticipated to be hot in the UK [59]. The reduced annual cooling energy demand in 2035 compared to 2025 is evidenced through the blue-ish tint of houses in 2035 and the red-yellow tint in 2025 in Figs. 16(a) and 16(b). These findings indicate that there may not be a yearly monotonous increase in cooling demand in the future. Atmospheric events like El Niño can intermittently affect cooling demand from year to year. However, the relative cooling demand among houses remained mostly consistent in both years under consideration, which was indicated by similar colour gradients across different houses in Figs. 16(a) and 16(b).

3.2. Parametric analysis for cooling load mitigation

Different active and passive cooling strategies to mitigate cooling demand were investigated to demonstrate the capabilities of the community model implemented in Modelica. The effect of cooling setpoint temperature was investigated first by considering two different setpoint values (22.5°C and 24°C) in addition to the base case setpoint temperature of 21°C. Subsequently, further possibilities of cooling load mitigation were analysed by relaxing certain active cooling system parameters. These included adopting a higher cooling air supply temperature of 16°C (against the base case with 10°C) and a lower maximum air flow rate of 2 ACH (against the base case with 4 ACH). Additionally, passive cooling intervention was investigated by adopting blind control schemes where the blinds were opened by 40%, 30%, and 20% of the window area when the indoor temperature rose above 22°C. Year 2025 was considered for this analysis as it involved higher cooling demand than 2035. Key results are shown in this section, with a critical discussion on the effects of these strategies on cooling demand of individual houses and the community being presented in Appendix C for the interested readers.

The difference in cooling demand across the houses within the community reduced upon the implementation of the energy-saving initiatives. This is evidenced through the box plots in Fig. 17, which show the distribution of annual cooling demand under the different mitigation scenarios. The thinner boxes in the plot represent smaller deviations among the annual cooling demand of the different houses. The reduced disparity in demand across households could be key towards establishing energy equality within the community [60].

3.3. Impact of energy-saving initiatives on cooling demand profiles

The cooling load mitigation strategies discussed in the previous section not only reduced the net annual cooling demand of the houses and the community but also influenced their cooling demand profiles. Fig. 18 shows the cooling demand profiles of the houses presented earlier in Fig. 14 after the implementation of the energy-saving strategies of higher cooling setpoint temperature (24°C) and blind opening by 30% for indoor temperatures above 22°C. The conservative settings of air supply (16°C and 2 ACH) were adopted to match the reduced cooling demand, although these settings do not have a pronounced effect. Year 2025 was considered for this assessment. The *y*-axis limits in Fig. 18 were kept the same as those of Fig. 14 to clearly appreciate the effects of the mitigation strategies.

The impacts of the cooling load mitigation strategies are evidenced in Fig. 18 through the lower peaks and shorter annual span of cooling

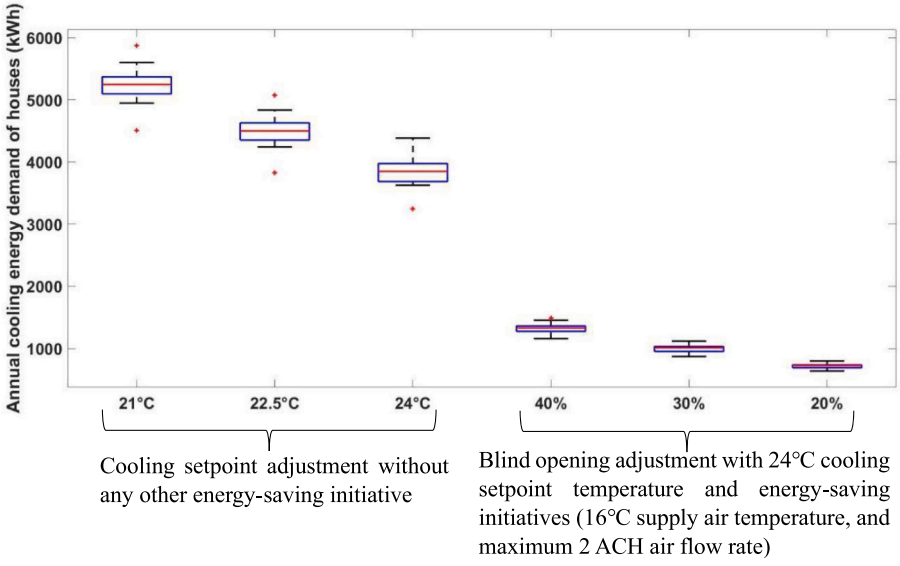

Fig. 17. Distribution of annual cooling demand of houses for different mitigation scenarios.

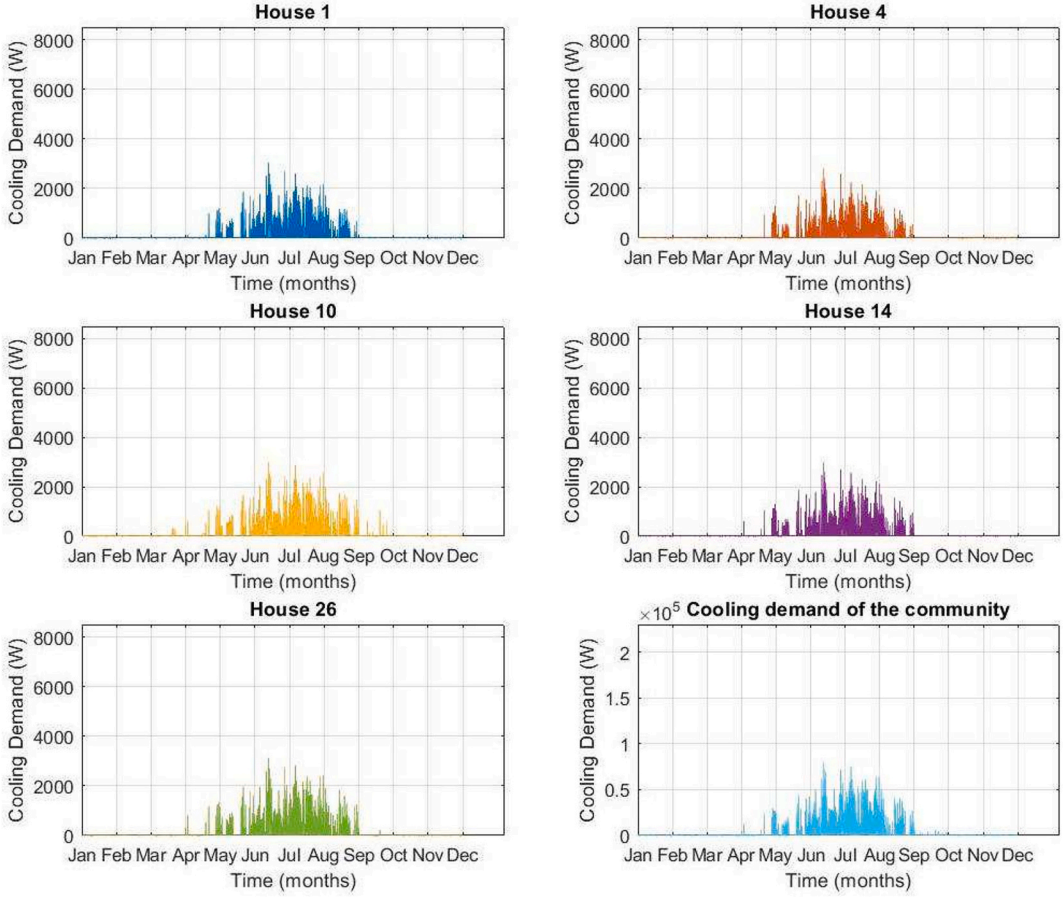

Fig. 18. Cooling demand profiles for different houses and the community for the year 2025 after the implementation of load-mitigation startegies.

demand for the different houses and the community itself. Furthermore, cooling demand in House 10 during winter months also disappeared. Similar impacts were observed for year 2035, but these are not shown here for the sake of brevity of the paper.

4. Limitations of the model

The reliance of the community model on external weather data presents a potential limitation. While obtaining ambient temperature profiles from credible sources like UKCP is relatively straightforward, these projections may not be available for all geographic regions. Similarly, global horizontal radiation data can be sourced from meteorological websites, but determining hourly incident radiation on each wall of a house, accounting for its shape, orientation, and shading from neighbouring structures requires dedicated design tools like IES VE, DesignBuilder, PVLIB, RADIANCE, SAM, or Google Sketchup, which may not be easily accessible to everyone. However, neglecting shading effects and simplifying building form factors allows for estimating incident solar radiation on walls using equations involving solar and surface azimuth angles [61]. This approach can alleviate the dependence of the developed model on external software for simpler house architectures.

The houses in the community were assumed to be airtight and the air exchanges through the opening of windows were not modelled. While this could be a reasonable assumption in traditionally colder climates, for houses located in hot climates and extensively adopting open-window ventilation, the air exchange through windows would need to be modelled. Such air exchanges relate directly to the extent of window opening, instantaneous pressure gradients between indoor and outdoor environments, and the intensity and direction of wind in the outdoor environment. These parameters involve a high degree of uncertainty and therefore the determination of air exchange through windows may not be precise and straightforward.

A caveat in the execution of the community-level model is that OpenModelica's parallel processing capabilities are still under development. A straightforward option to distribute model execution load across available parallel processors in the machine is not yet available under the simulation settings tabs in the GUI of the software. This could represent an issue when simulating a housing community with several dwellings. There is an option in the software to allocate multiple processors for compiling the models, but to realise substantial gains in computational speed, parallel processing in model execution is required. This feature may be integrated as a straightforward option in future versions of the software, but assessing this falls out of the scope of this paper.

Due to constraints in parallel processing of the large community-level model, this was simulated by considering smaller batches of houses in one simulation run. For example, the first instance of the community model simulated Houses 1 to 11, the second instance simulated Houses 12 to 22, and the third instance simulated Houses 23 to 31. This approach is shown in Appendix A.

5. Conclusions

To better understand and quantify the requirements for cooling infrastructure in the UK's residential sector under the effects of climate change, this paper presented the development of an open-source tool for estimating cooling demand in a housing community. The tool facilitated insights into how individual houses and a community as a whole can experience overheating and how the cooling demand is distributed

across different households within the community under investigation. The tool was developed using a bottom-up approach employing three levels of design hierarchy within the Modelica platform.

At the fundamental design level, the tool allowed for the modelling of house envelope components such as walls, roofs, doors, and windows. This level supported passive interventions for reducing cooling demand, such as various blind control schemes. The intermediate design level combined the components developed at the fundamental level with a cold air supply system to quantify the cooling demand of individual houses. This level offered controls for active cooling measures, enabling adjustments to cooling setpoint temperature, cold air supply temperature, and cold air flow rate to cater for the unmet cooling demand after passive interventions. The top design level aggregated the cooling demand for all houses in a community and incorporated internal heat gain profiles and weather parameters, enabling assessments of the impact of different weather conditions, such as temperature forecasts for future years on community cooling demand.

The cooling demand for houses with similar architecture varied significantly based on their locations and orientations within the community, especially when active cooling systems were heavily relied upon. For instance, in year 2025, the annual cooling demand for different houses in the community ranged from 4505.8 kWh to 5873.4 kWh, with potential implications for energy bills of households. This indicates that prospective decisions on house acquisition would benefit from understanding the potential energy consumption for space cooling alongside aesthetics and general accessibility within a community.

Furthermore, the adoption of strategies, such as higher cooling setpoint temperatures and blind controls could significantly mitigate cooling loads and reduce disparities in cooling demand across houses. Collectively applying these cooling load mitigation strategies reduced the range of annual cooling demand for different houses to 634.8 kWh - 797.7 kWh.

The cooling demand of both individual houses and the entire community was significantly influenced by ambient temperature projections for the years under consideration. The forecast of higher ambient temperatures in 2025 than in 2035 resulted in increased community cooling demand in 2025. Atmospheric events may lead to an intermittent increase in cooling demand for housing communities rather than a consistent upward trend.

CRediT authorship contribution statement

Pranaynil Saikia: Writing – original draft, Visualization, Validation, Software, Methodology, Investigation, Formal analysis, Data curation. **Lloyd Corcoran:** Writing – original draft, Validation, Software, Methodology, Investigation, Data curation. **Carlos E. Ugalde-Loo:** Writing – review & editing, Supervision, Resources, Project administration, Methodology, Funding acquisition, Conceptualization. **Muditha Abeysekera:** Supervision, Resources, Project administration, Conceptualization.

Declaration of competing interest

The authors declare that they have no known competing financial interests or personal relationships that could have appeared to influence the work reported in this paper.

Data availability

The cooling demand estimator is open-sourced as supplementary material provided alongside this paper. The same is also made available in the Cardiff University data repository at https://doi.org/10.17035/cardiff.27160632.

Acknowledgements

The work presented in this paper was supported by the Engineering and Physical Sciences Research Council (EPSRC), UK Research and Innovation, through the project ‘Flexibility from Cooling and Storage (Flex-Cool-Store)’ under grant EP/V042505/1. The work was also supported jointly by the UK-India Education and Research Initiative (UKIERI), British Council, UK, and the Scheme for Promotion of Academic and Research Collaboration (SPARC), India, through the project ‘Advancing Sustainable Building Practices: A Comprehensive Investigation into Estimation Techniques for Thermal Load of Buildings’ under grant numbers UKIERI-SPARC/03/11 (UK) and SPARC-UKIERI/2024-2025/P3094 (India). The authors thank the Advanced Research Computing team at Cardiff University for helping with the computational resources during the development of the research work.

Appendix A

This appendix contains the figures for the models developed in Modelica and used in different levels of modelling hierarchy. These were not presented in Section 2 of the paper for the sake of brevity.

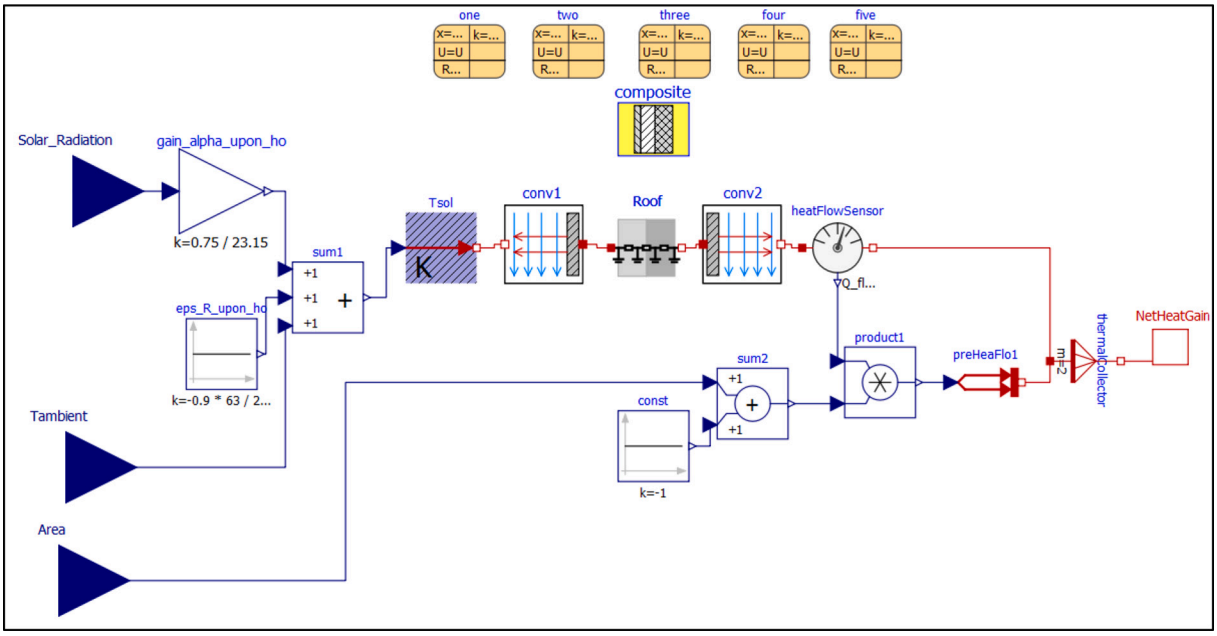

Fig. A1. Screenshot of the roof model implementation in Modelica.

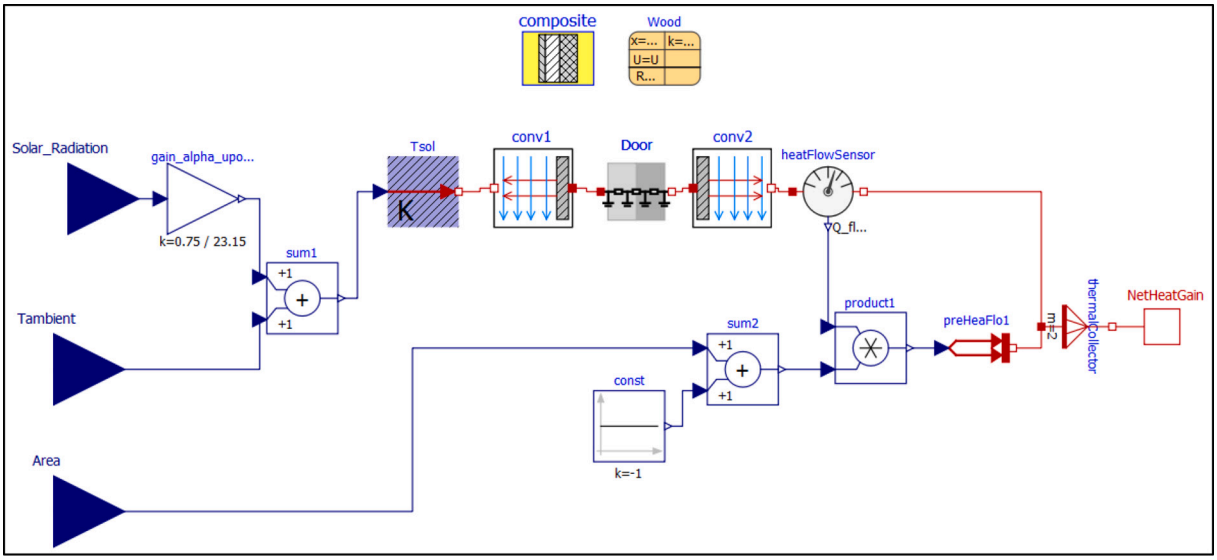

Fig. A2. Screenshot of the door model implementation in Modelica.

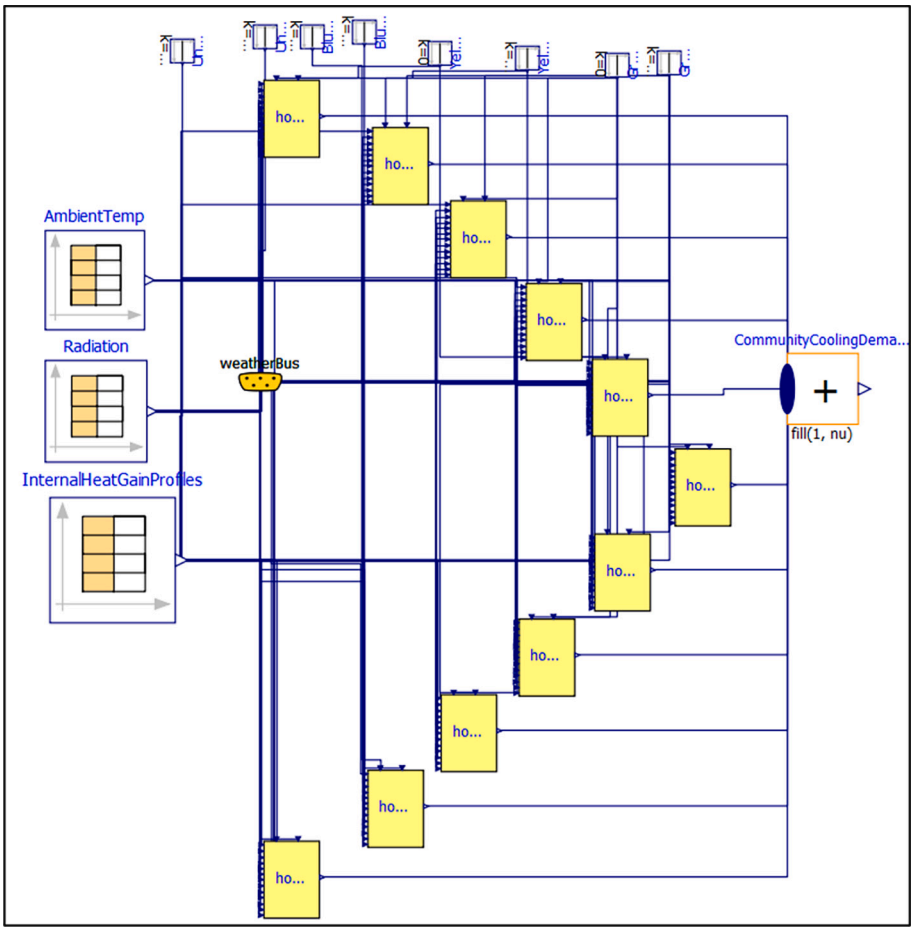

Fig. A3. Screenshot of the community-level cooling demand model in Modelica (Houses 1–11).

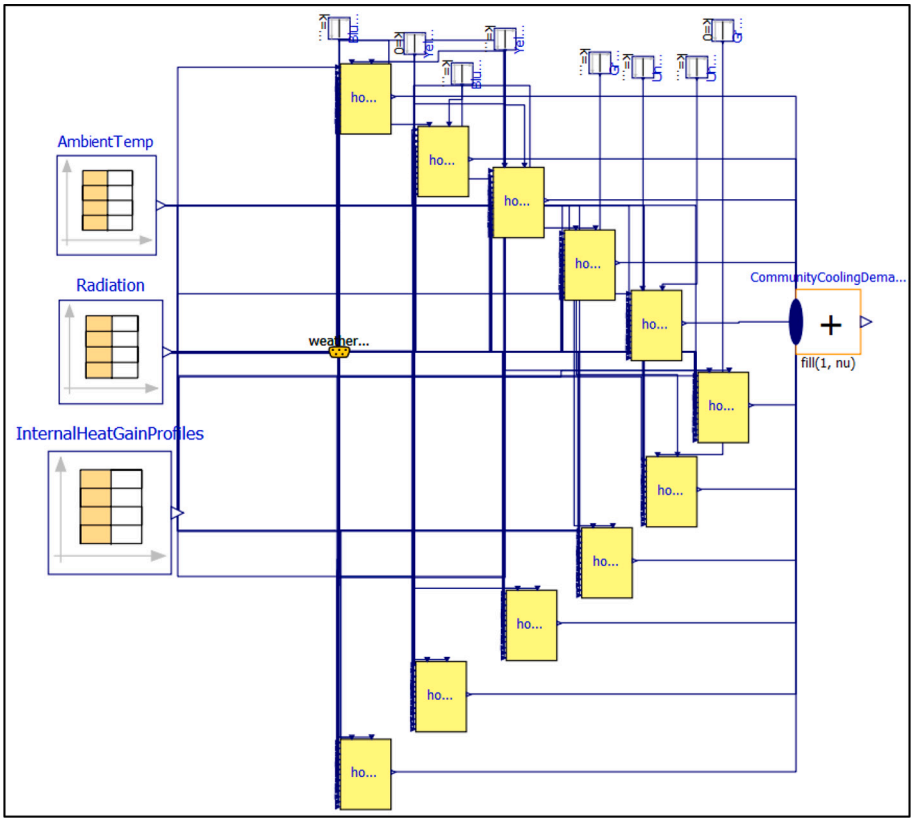

Fig. A4. Screenshot of the community-level cooling demand model in Modelica (Houses 12–22).

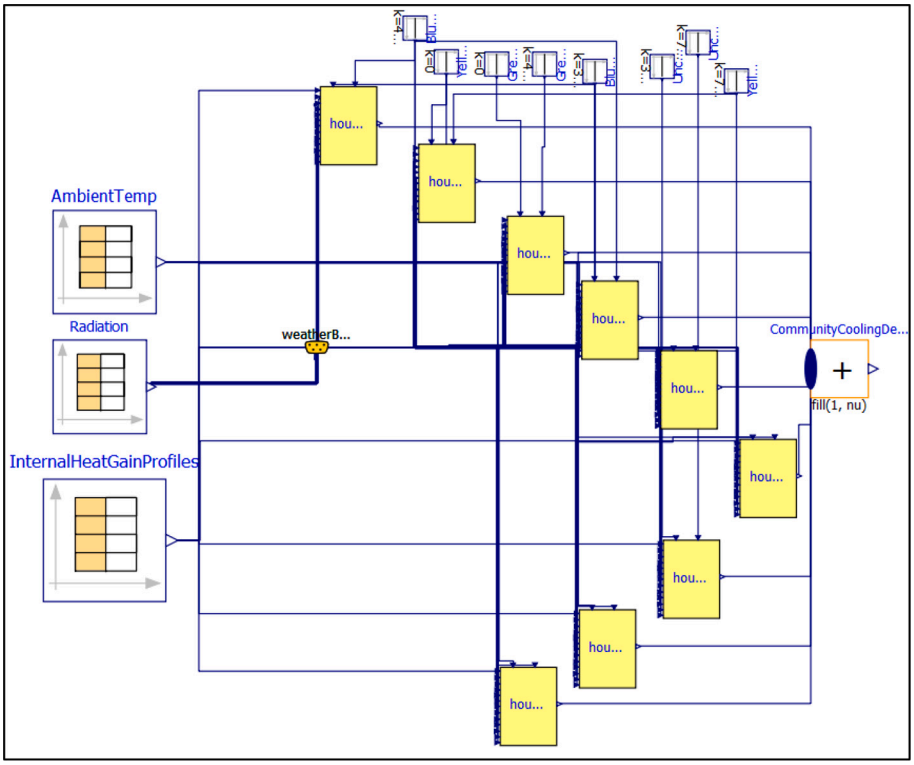

Fig. A5. Screenshot of the community-level cooling demand model in Modelica (Houses 23–31).

Appendix B

This appendix provides the cooling demand profiles for the houses in the community, which were not presented in Section 3.1 of the paper. The

settings of the base case with 21°C cooling setpoint temperature, 10°C cold air supply temperature with a maximum flow rate of 4 ACH, and completely open blinds were considered for generating these profiles.

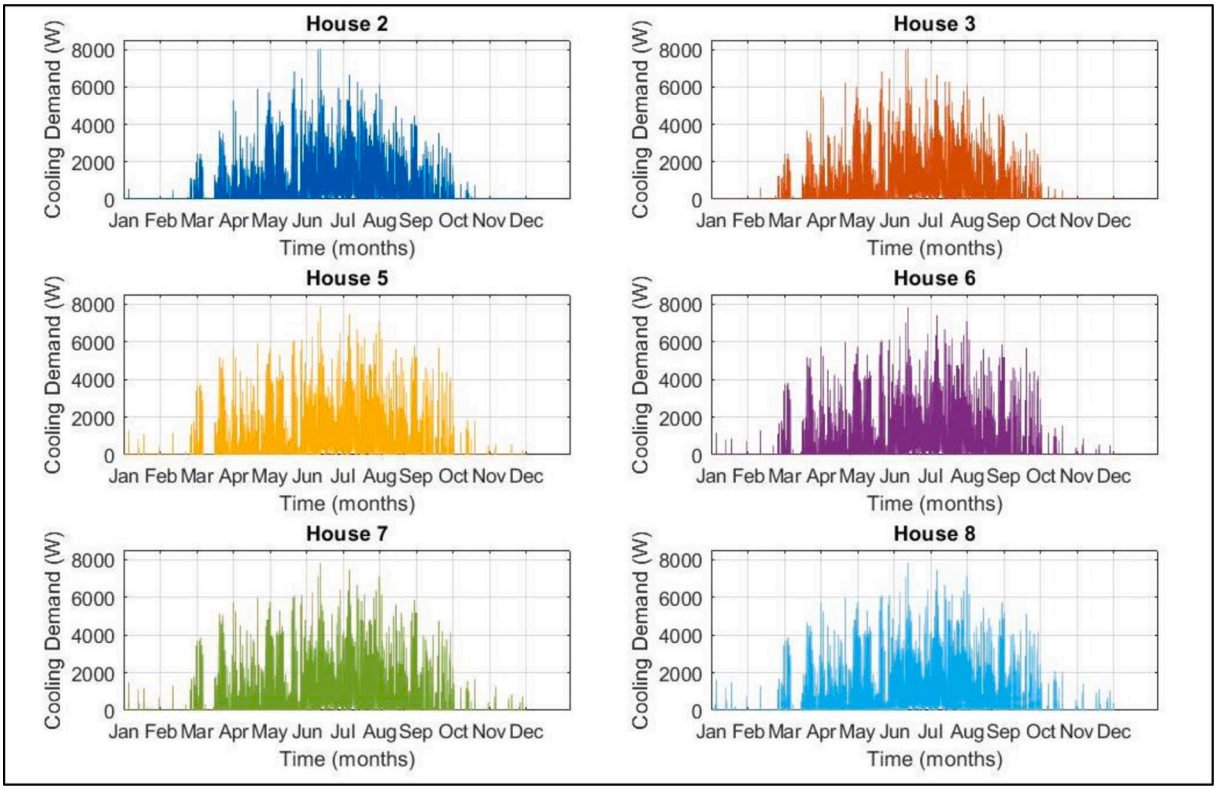

Fig. B1. Cooling demand profiles for Houses 2, 3, 5, 6, 7, and 8 (year 2025).

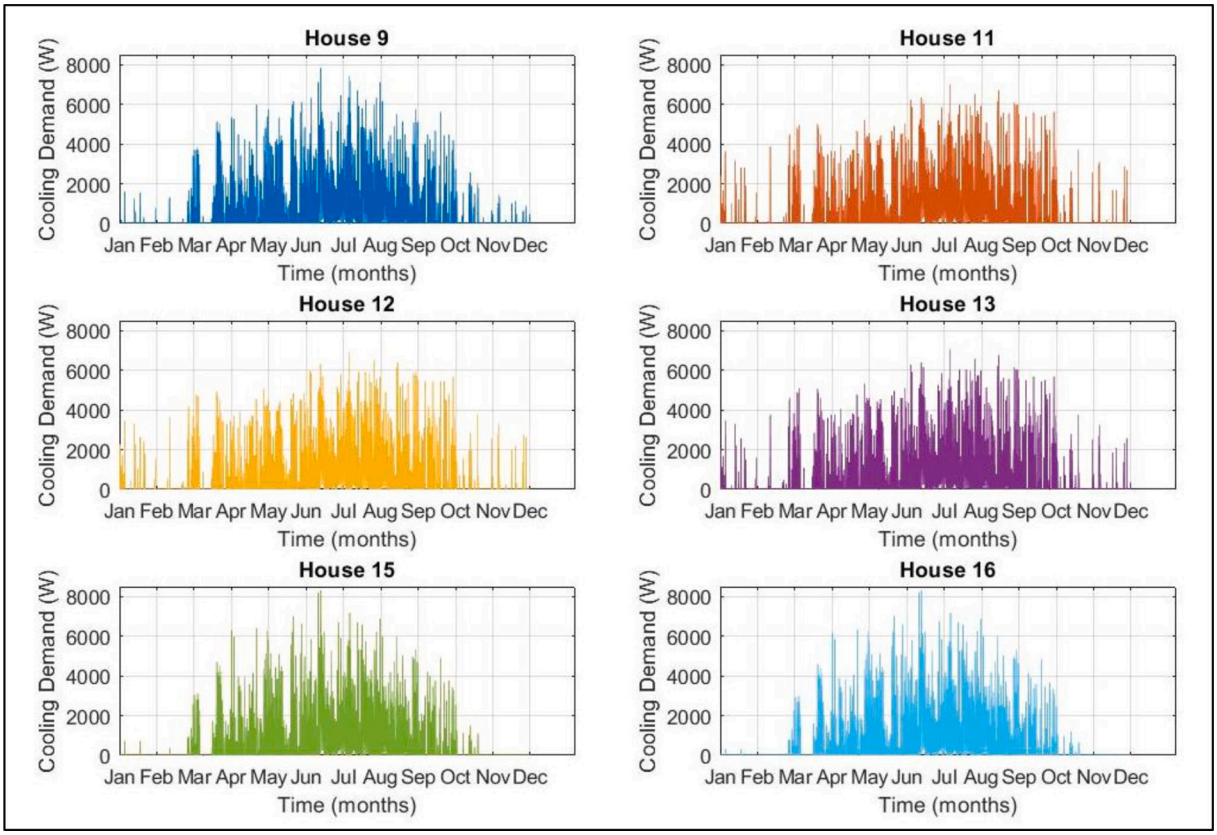

Fig. B2. Cooling demand profiles for Houses 9, 11, 12, 13, 15, and 16 (year 2025).

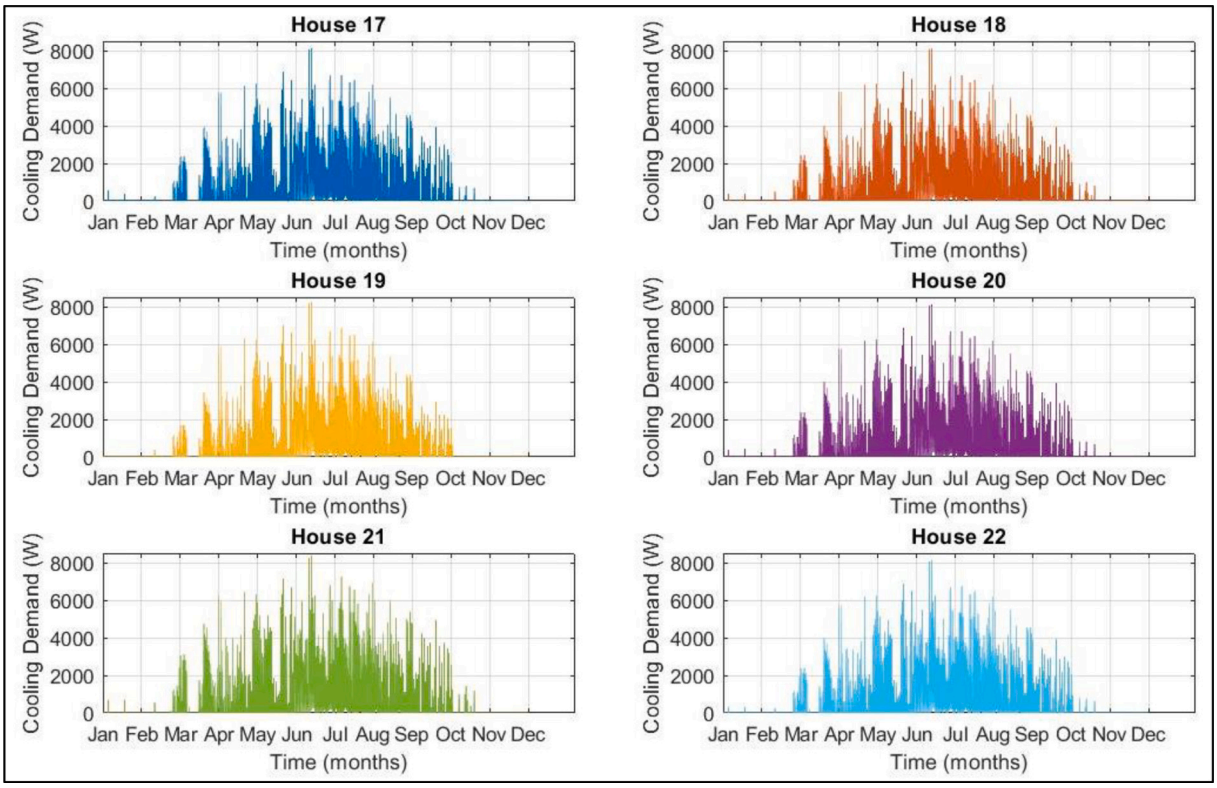

Fig. B3. Cooling demand profiles for Houses 17, 18, 19, 20, 21, and 22 (year 2025).

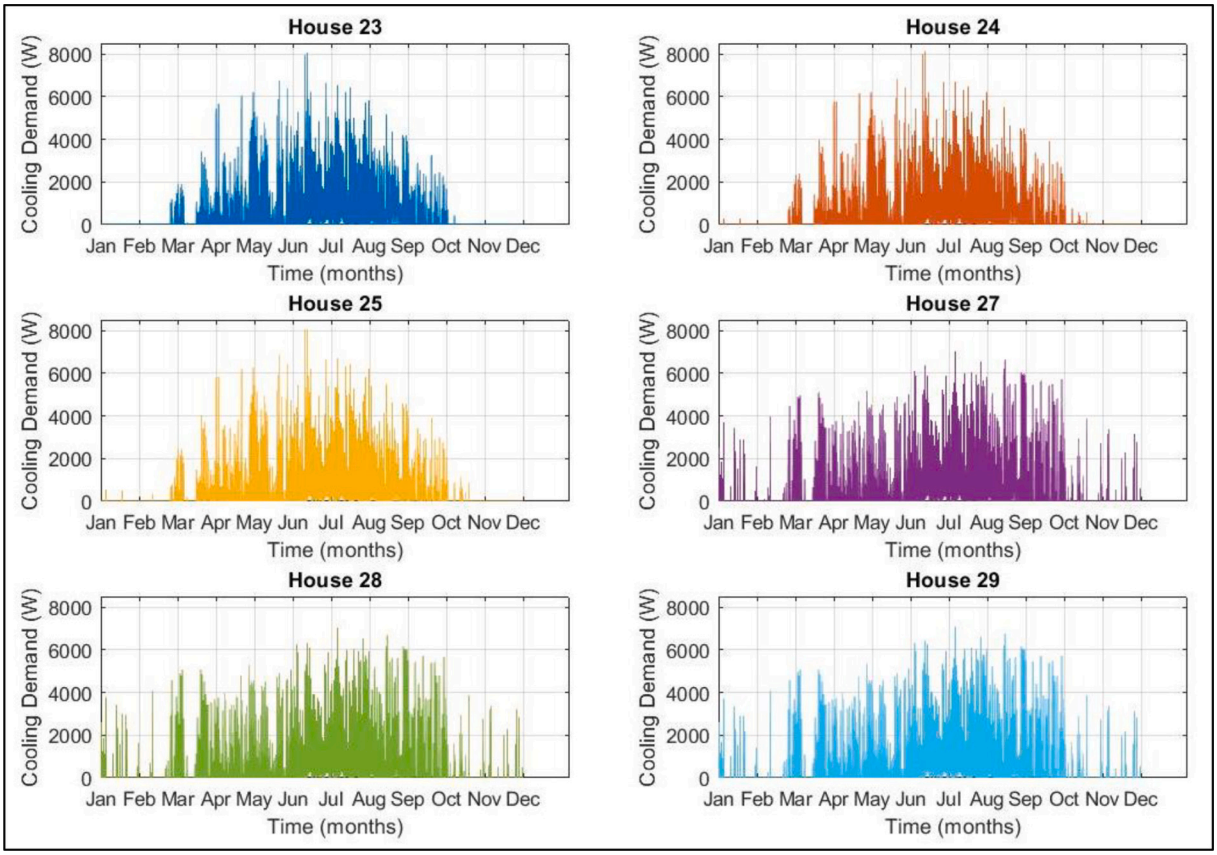

Fig. B4. Cooling demand profiles for Houses 23, 24, 25, 27, 28, and 29 (year 2025).

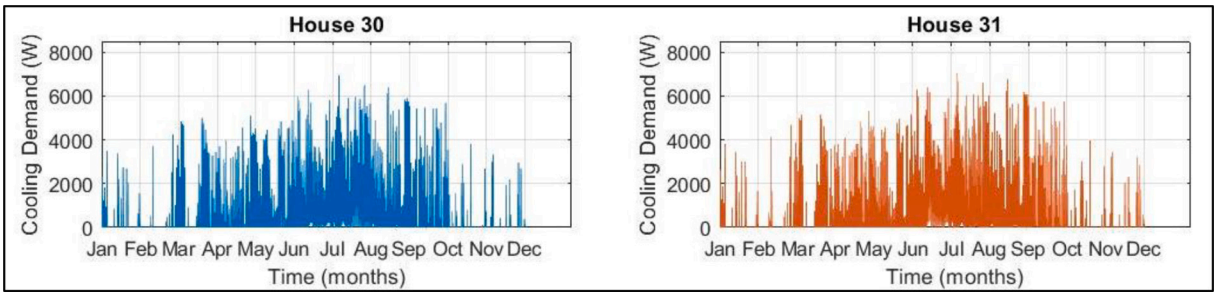

Fig. B5. Cooling demand profiles for Houses 30 and 31 (year 2025).

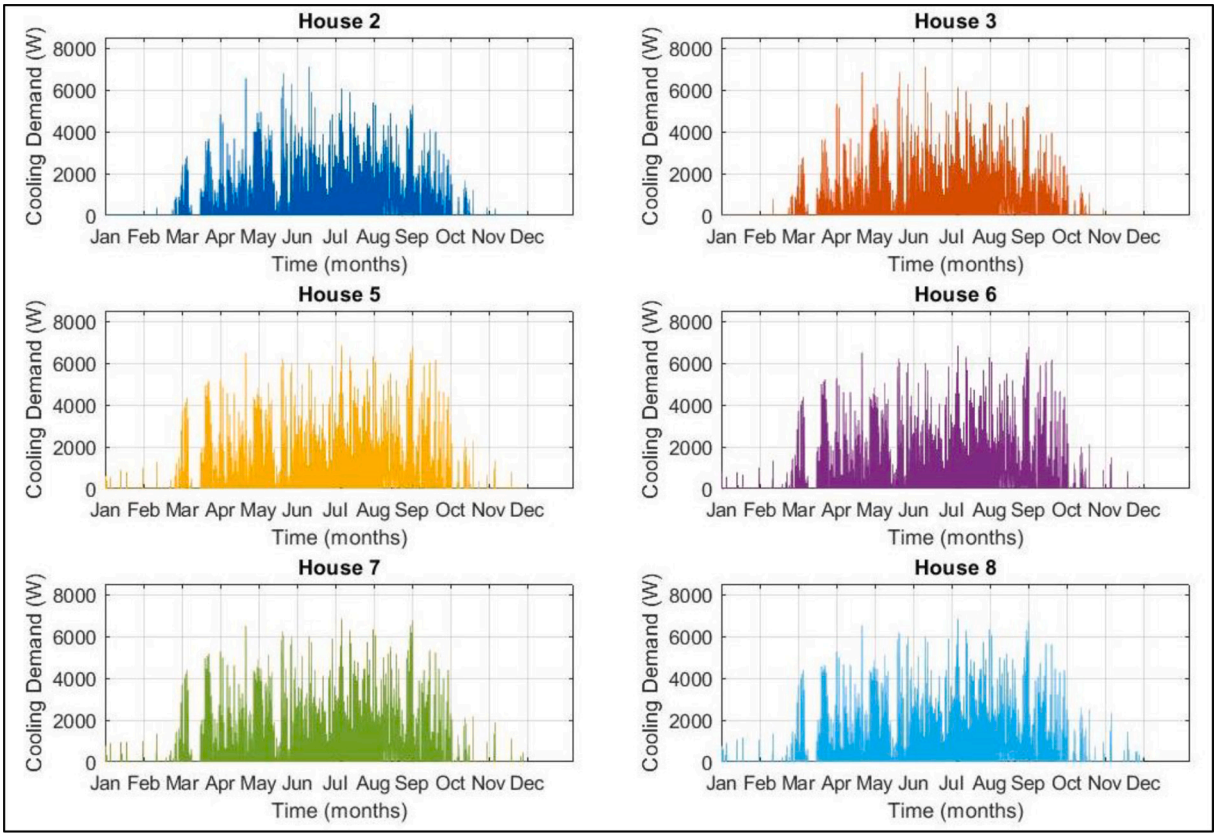

Fig. B6. Cooling demand profiles for Houses 2, 3, 5, 6, 7, and 8 (year 2035).

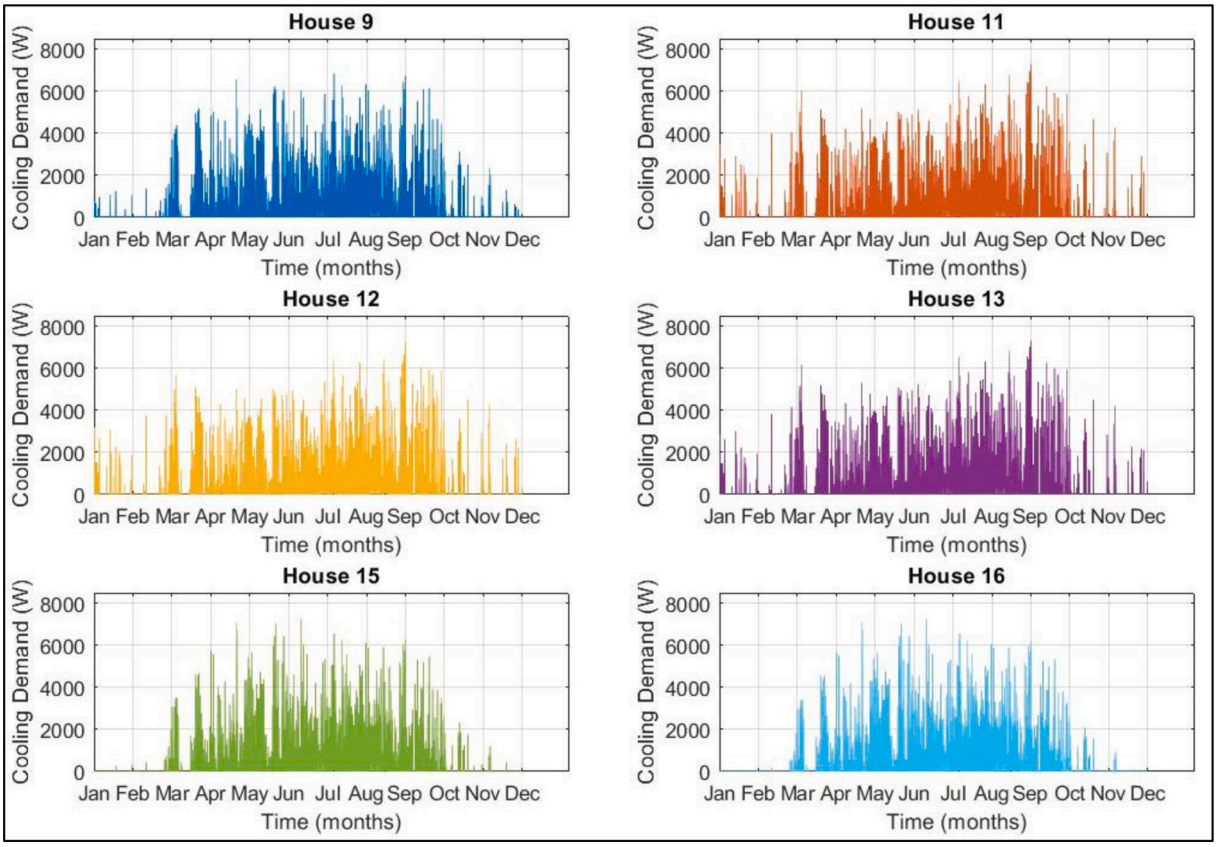

Fig. B7. Cooling demand profiles for Houses 9, 11, 12, 13, 15, and 16 (year 2035).

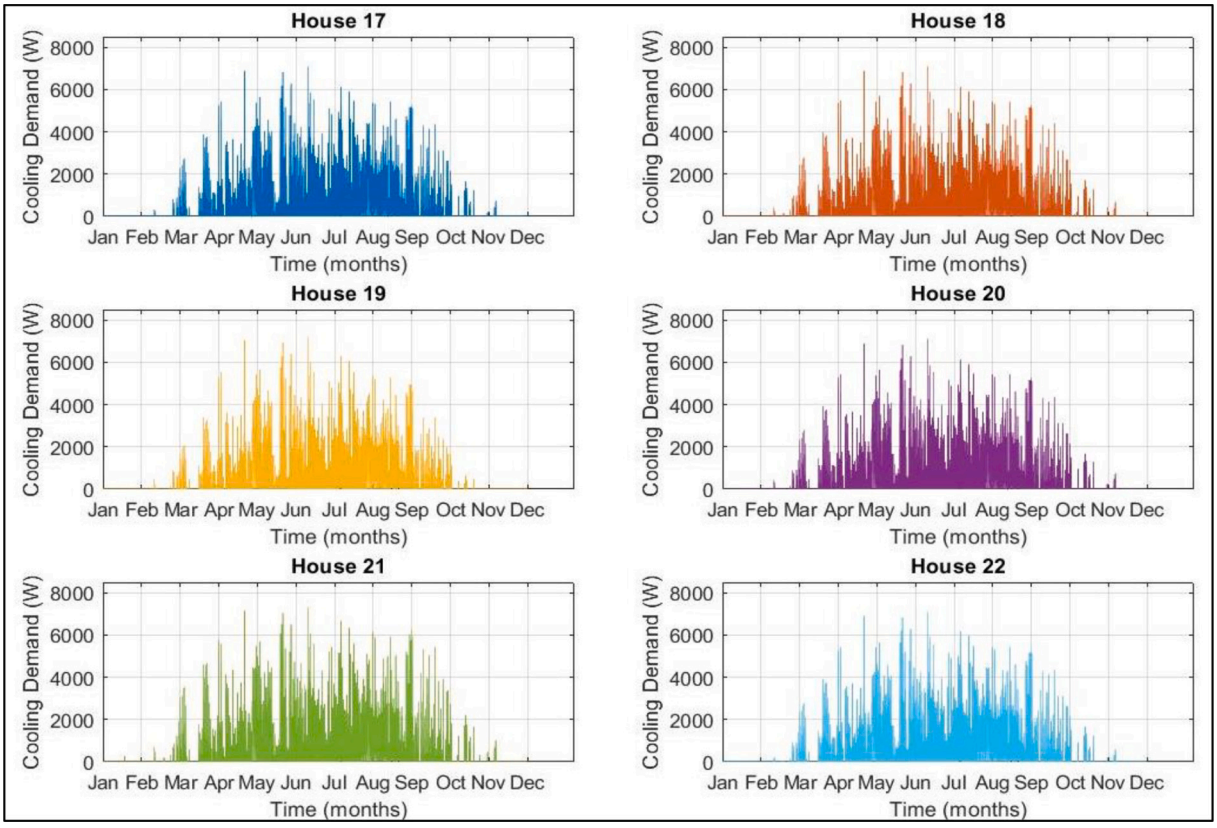

Fig. B8. Cooling demand profiles for Houses 17, 18, 19, 20, 21, and 22 (year 2035).

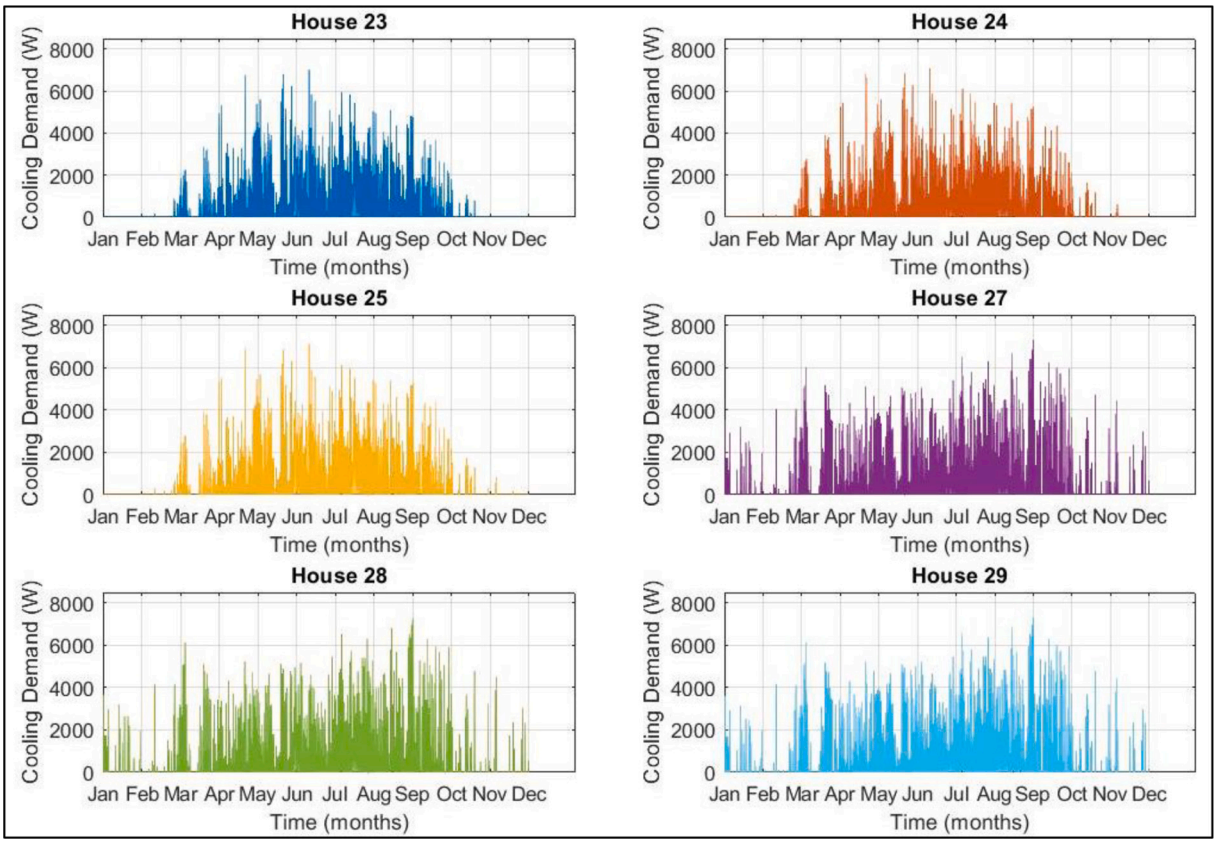

Fig. B9. Cooling demand profiles for Houses 23, 24, 25, 27, 28, and 29 (year 2035).

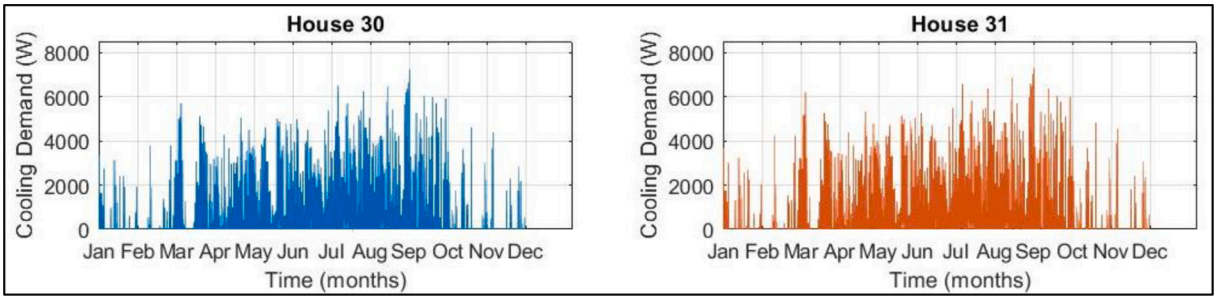

Fig. B10. Cooling demand profiles for Houses 30 and 31 (year 2035).

Appendix C

This appendix provides a detailed analysis and discussion on the effects of different cooling load mitigation strategies assessed under Section 3.2 of the paper.

C.1. Effect of different cooling setpoint temperatures

Two different cooling setpoint temperatures (22.5°C and 24°C) were considered for this analysis. The community model was simulated to quantify the cooling demand for these setpoint values.

Fig. C1 shows the annual cooling demand of different houses within the community for the setpoint temperatures using a radar chart. Annual cooling demand was within 5000–6000 kWh for a setpoint temperature of 21°C. The cooling demand ranges reduced to 4000–5000 kWh for 22.5°C and 3500–4500 kWh for 24°C. These results indicate how marginal changes in the operational settings of the building cooling system could result in significant changes in energy consumption. Such information may be instrumental to sensitise home-owners on how minor adjustments in comfort levels can lead to substantial energy savings.

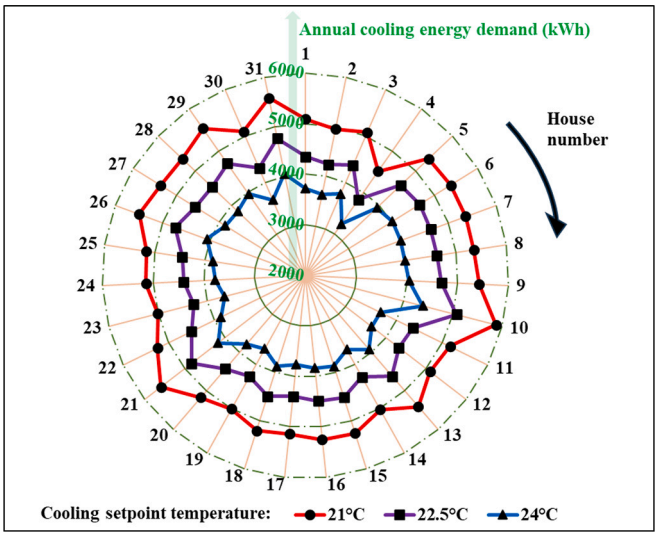

Fig. C1. Annual cooling demand of different houses with different cooling setpoint temperatures.

Setpoint adjustments can lead to an even more pronounced impact on the community-level cooling demand. Fig. C2 shows that a cooling demand reduction of ~20 MWh could be achieved by increasing cooling setpoint temperatures by 1.5°C in the houses.

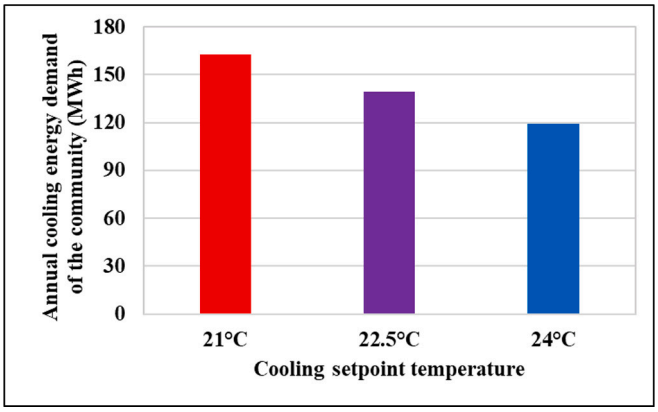

Fig. C2. Annual cooling demand of the community for different cooling setpoint temperatures.

C.2. Effect of blind control strategies on cooling demand

A cooling setpoint temperature of 24°C, which yielded the minimum cooling demand in Section C.1, was here adopted to explore further demand reduction by implementing a blind control scheme where the blinds were opened by 40 %, 30 %, and 20 % of the window area when the indoor temperature rose above 22°C. The higher cooling setpoint along with blind operation was deemed to reduce the cooling demand significantly. Therefore, a conservative mode of the air supply system was adopted which included setting the supply air temperature to a higher value of 16°C and reducing the maximum supply air flow rate to 2 ACH. The results obtained after simulating the community model with these additional mitigation approaches are shown in Figs. C3 and C4.

Fig. C3 evidences a significant reduction in cooling demand of the houses when the additional energy-saving initiatives are incorporated. Prior to their implementation, the annual cooling demand of the houses was in the range of 3500–4500 kWh (see the blue trace in Fig. C1). With the energy-saving measures, demand was capped under 1600 kWh for every house. Depending upon the percentage of blind opening, the annual cooling demand could be capped to ~1600 kWh for 40 %, ~1200 kWh for 30 %, and ~ 800 kWh for 20 % (see the three concentric traces in Fig. C3). These results emphasise how a strategic approach to active and passive measures is favourable towards mitigating cooling demand at its source. Fig. C4 shows that the impact of a blind opening scheme alone could amount to ~10 MWh at the community level cooling demand over an annual time horizon.

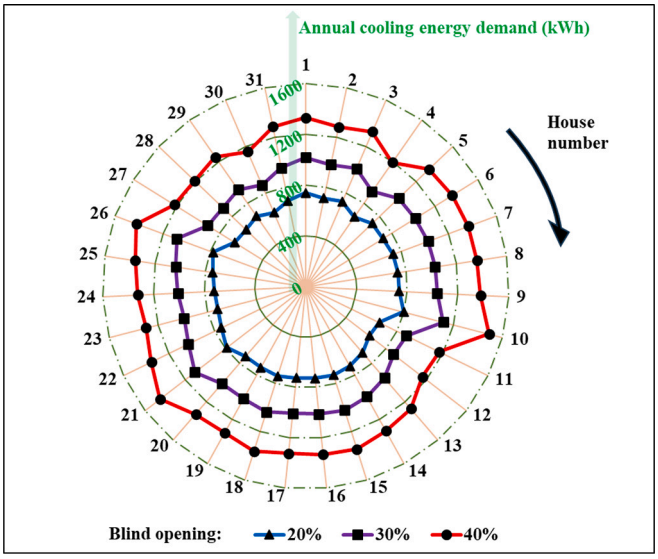

Fig. C3. Annual cooling demand of different houses with the adoption of energy-saving initiatives.

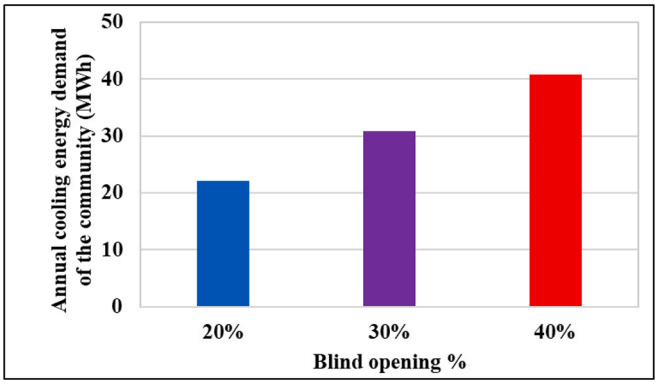

Fig. C4. Annual cooling demand of the community for different blind openings.

C.3. Effect of supply air temperature and maximum flow rate on cooling demand

While Figs. C3 and C4 in Section C.2 demonstrate how different blind opening schemes significantly impact the cooling load of houses and the community, the effects of increased supply air temperature and reduced maximum air flow rate are not immediately apparent in these figures. Consequently, an additional analysis was conducted to explicitly examine the impact of supply air temperature and maximum air flow rate on cooling demand. For this analysis, the intermediate case of blind opening by 30% was adopted along with a cooling setpoint temperature of 24°C for year 2025. Two sets of supply air temperature and maximum air flow rate were considered: one with the settings for the base case (10°C and 4 ACH), and the other with the conservative settings (16°C and 2 ACH) adopted in Section C.2.

The annual cooling demand for the different houses, based on the two air supply settings, showed only marginal variations, as evidenced in Fig. C5. These small differences could be attributed to: (a) variations resulting from numerical computations and round-off approximations at different time-steps for the two cases, and (b) minor variations in the operation of the air flow control valve, which handled the different supply air attributes, leading to slight changes in indoor temperature variations. These variations may have affected the rate of heat flow to and from the outdoor environment. Both supply air configurations were able to maintain the indoor air temperature within the cooling setpoint throughout the year for most of the houses. However, for House 10, described in Section 3.1, which had the highest cooling demand due to high sun exposure and minimal shading from neighbouring houses, the conservative air supply settings were insufficient to compensate for the high heat gain. As a result, the indoor temperature exceeded the cooling setpoint on several occasions during summer. (These results are not included in the paper for the sake of brevity but can be easily generated by the interested readers by executing the source code provided in the supplementary material.)

Following these observations, it can be inferred that while supply air temperature and maximum flow rate may not impact the overall cooling demand, a larger capacity supply air system — capable of delivering lower inlet temperatures and higher flow rates — may be necessary for houses with low cooling setpoint temperatures, high sun exposure, and no passive mitigation measures such as blind operation.

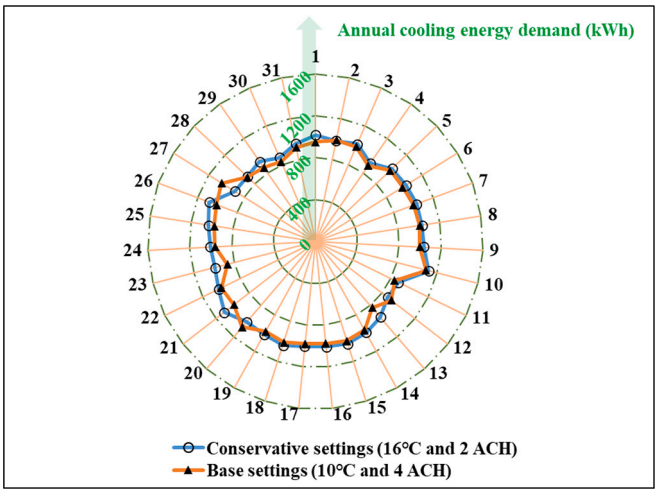

Fig. C5. Comparison of the annual cooling demand for conservative and base case settings of supply air temperature and maximum air flow rate.

Supplementary data

Supplementary data to this article can be found online at https://doi.org/10.1016/j.apenergy.2024.124597.

References

[1] How climate change worsens heatwaves, droughts, wildfires and floods - BBC news. 2024. https://www.bbc.co.uk/news/science-environment-58073295 (accessed July 2, 2024).

[2] How does climate change affect the strength and frequency of floods, droughts, hurricanes, and tornadoes? | Royal Society. 2020. https://royalsociety.org/news-resources/projects/climate-change-evidence-causes/question-13/ (accessed July 2, 2024).

[3] UK is no longer a cold country and must adapt to heat, say climate scientists | Climate crisis | The Guardian. 2022. https://www.theguardian.com/environment/2022/jul/18/uk-weather-heatwave-cold-country-adapt-heat-climate (accessed October 23, 2023).

[4] Is climate change causing the heatwave? Here's the simple science behind Europe's worrying weather | Euronews. 2022. https://www.euronews.com/green/2022/07/29/is-climate-change-causing-the-heatwave-heres-the-simple-science-behind-europes-scorching-w (accessed October 23, 2023).

[5] Climate change impacts of heat and cold extremes on humans. 2020.

[6] Net zero strategy: build back greener. 2021.

[7] 2050 long-term strategy. https://climate.ec.europa.eu/eu-action/climate-strategies-targets/2050-long-term-strategy_en (accessed October 23, 2023).

[8] Five things you need to know about: decarbonising Europe | Research and Innovation. 2019. https://ec.europa.eu/research-and-innovation/en/horizon-magazine/five-things-you-need-know-about-decarbonising-europe (accessed November 6, 2023).

[9] Sustainable cooling: postnote. 2021. https://researchbriefings.files.parliament.uk/documents/POST-PN-0642/POST-PN-0642.pdf.

[10] Heat resilience and sustainable cooling Fifth Report of Session 2023–24 Report, with an Appendix, together with formal minutes relating to the report. 2024.

[11] Corcoran L, Saikia P, Ugalde-Loo CE, Abeysekera M. Methodology to quantify cooling demand in typical UK dwellings. Energy Procedia 2024:42. https://doi.org/10.46855/ENERGY-PROCEEDINGS-10996.

[12] Ugalde-Loo CE. Are we prepared to cool down in a warming world? Oxford Energy Forum 2022;134:47–50.

[13] Khosravi F, Lowes R, Ugalde-Loo CE. Cooling is hotting up in the UK. Energy Policy 2023;174:113456. https://doi.org/10.1016/J.ENPOL.2023.113456.

[14] Gonzalo DA, Santamaría M, Montero Burgos B, Caggiano A, Portnov BA, Del F, et al. Assessment of Building Energy Simulation Tools to Predict Heating and Cooling Energy Consumption at Early Design Stages. Sustain15; 2023. https://doi.org/10.3390/SU15031920. Page 1920 2023;15:1920.

[15] Mousavi SN, Gheibi M, Wacławek S, Smith NR, Hajiaghaei-Keshteli M, Behzadian K. Low-energy residential building optimisation for energy and comfort enhancement in semi-arid climate conditions. Energy Convers Manag 2023;291:117264. https://doi.org/10.1016/J.ENCONMAN.2023.117264.

[16] Anter AG, Sultan AA, Hegazi AA, el Bouz MA. Thermal performance and energy saving using phase change materials (PCM) integrated in building walls. J Energy Storage 2023;67:107568. https://doi.org/10.1016/J.EST.2023.107568.

[17] Saikia P, Rakshit D, Narayanaswamy R, Wang F, Udayraj.. Energy performance and indoor airflow analysis of a healthcare ward designed with resource conservation objectives. J Build Eng 2021;44:103296. https://doi.org/10.1016/J.JOBE.2021.103296.

[18] Khalid H, Thaheem MJ, Malik MSA, Musarat MA, Alaloul WS. Reducing cooling load and lifecycle cost for residential buildings: a case of Lahore. Pakistan Int J Life Cycle Assess 2021;26:2355–74. https://doi.org/10.1007/S11367-021-02000-1/FIGURES/4.

[19] Krüger E, Pearlmutter D, Rasia F. Evaluating the impact of canyon geometry and orientation on cooling loads in a high-mass building in a hot dry environment. Appl Energy 2010;87:2068–78. https://doi.org/10.1016/J.APENERGY.2009.11.034.

[20] Alshenaifi MA, Sharples S, Abuhussain MA, Alotaibi BS, Aldersoni AA, Abdelhafez MHH. Integrating a passive downdraught evaporative cooling tower into a Saudi house - the impact of climatic conditions on PDEC performance. Build Environ 2023;242:110497. https://doi.org/10.1016/J.BUILDENV.2023.110497.

[21] Corcoran L, Saikia P, Ugalde-Loo CE, Abeysekera M. An effective methodology to quantify cooling demand in the UK housing stock. Appl Energy 2024 (under review).

[22] Corcoran L, Ugalde-Loo CE, King L, Demski C. Analysing the effects of common passive cooling strategies in UK homes. Int Conf Appl Energy Niigata City Jpn 2024. p. (accepted).

[23] Rashad M, Żabnieńska-Góra A, Norman L, Jouhara H. Analysis of energy demand in a residential building using TRNSYS. Energy 2022;254:124357. https://doi.org/10.1016/J.ENERGY.2022.124357.

[24] Saleem A, Ugalde-Loo CE. Thermal performance analysis of a heat pump-based energy system to meet heating and cooling demand of residential buildings. Appl Energy 2024 (under review).

[25] Hinkelman K, Wang J, Zuo W, Gautier A, Wetter M, Fan C, et al. Modelica-based modeling and simulation of district cooling systems: a case study. Appl Energy 2022;311:118654. https://doi.org/10.1016/J.APENERGY.2022.118654.

[26] Zhang W, Jin X, Zhang L, Hong W. Performance of the variable-temperature multi-cold source district cooling system: a case study. Appl Therm Eng 2022;213:118722. https://doi.org/10.1016/J.APPLTHERMALENG.2022.118722.

[27] Huang S, Wang J, Fu Y, Zuo W, Hinkelman K, Kaiser RM, et al. An open-source virtual testbed for a real net-zero energy community. Sustain Cities Soc 2021;75:103255. https://doi.org/10.1016/J.SCS.2021.103255.

[28] Qiu K, Yang J, Gao Z, Xu F. A review of Modelica language in building and energy: development, applications, and future prospect. Energy Build 2024;308:113998. https://doi.org/10.1016/J.ENBUILD.2024.113998.

[29] Zou M, Huang W, Jin J, Hu B, Liu Z. Deep spatio-temporal feature fusion learning for multi-step building cooling load forecasting. Energy Build 2024;322:114735. https://doi.org/10.1016/J.ENBUILD.2024.114735.

[30] Prataviera E, Romano P, Carnieletto L, Pirotti F, Vivian J, Zarrella A. EUReCA: An open-source urban building energy modelling tool for the efficient evaluation of cities energy demand. Renew Energy 2021;173:544–60. https://doi.org/10.1016/J.RENENE.2021.03.144.

[31] UKCP data - met office. https://www.metoffice.gov.uk/research/approach/collaboration/ukcp/data/index (accessed October 23, 2023).

[32] CIBSE. Weather data. https://www.cibse.org/weatherdata (accessed November 6, 2023).

[33] Software validation and approval | IES virtual environment. https://www.iesve.com/software/software-validation (accessed July 2, 2024).

[34] Solar radiation. https://help.iesve.com/ve2021/solar_radiation.htm (accssed October 23, 2023).
[35] Applications modelit. https://www.iesve.com/software/virtual-environment/modelit (accessed September 21, 2024).
[36] Shading devices. https://help.iesve.com/ve2021/shading_devices.htm (accessed September 21, 2024).
[37] Roberts BM, Abel B, Allinson D, Crowley J, Rashid T, Salehi B, et al. A dataset from synthetically occupied test houses for validating model predictions of overheating. CIBSE Tech. Symp.,. Loughborough University; 2022. https://doi.org/10.17028/RD.LBORO.19308299.
[38] What's the ideal room temperature for your home? | OVO Energy. 2024. https://www.ovoenergy.com/guides/energy-guides/average-room-temperature (accessed October 23, 2023).
[39] Plans unveiled to decarbonise UK power system by 2035 - GOV.UK n.d. 2021. https://www.gov.uk/government/news/plans-unveiled-to-decarbonise-uk-power-system-by-2035 (accessed October 23, 2023).
[40] Buildings.heattransfer.conduction. https://simulationresearch.lbl.gov/modelica/releases/v4.0.0/help/Buildings_HeatTransfer_Conduction.html#Buildings.HeatTransfer.Conduction.MultiLayer (accessed October 23, 2023).
[41] Saikia P, Rakshit D. Passive building cooling achieved with a new class of thermal retrofit: the liquid vapour phase change material. Energy Build 2021;249:111238. https://doi.org/10.1016/J.ENBUILD.2021.111238.
[42] Low zero carbon (LZC) feasibility Report. 2016.
[43] ApacheSim: construction database (APcdb) IESVE trial support material. 2020.
[44] Zhou D, Eames P. Phase change material wallboard (PCMW) melting temperature optimisation for passive indoor temperature control. Renew Energy 2019;139:507–14. https://doi.org/10.1016/J.RENENE.2019.02.109.
[45] Hwang RL, Chen WA. Identifying relative importance of solar design determinants on office building façade for cooling loads and thermal comfort in hot-humid climates. Build Environ 2022;226:109684. https://doi.org/10.1016/J.BUILDENV.2022.109684.
[46] Sharma P, Rakshit D. Quantitative assessment of orientation impact on heat gain profile of naturally cooled buildings in India. Adv Build Energy Res 2017;11:208–26. https://doi.org/10.1080/17512549.2016.1215261.
[47] Kang X, Yan D, Xie X, An J, Liu Z. Co-simulation of dynamic underground heat transfer with building energy modeling based on equivalent slab method. Energy Build 2022;256:111728. https://doi.org/10.1016/J.ENBUILD.2021.111728.
[48] McAdams WH. Heat transmission. Tokyo, Japan: McGraw-Hill Kogakusha; 1954.
[49] Mirsadeghi M, Cóstola D, Blocken B, Hensen JLM. Review of external convective heat transfer coefficient models in building energy simulation programs: implementation and uncertainty. Appl Therm Eng 2013;56:134–51. https://doi.org/10.1016/j.applthermaleng.2013.03.003.
[50] Annual average wind speed in the United Kingdom (UK) from 2001 to 2023. 2024. https://www.statista.com/statistics/322785/average-wind-speed-in-the-united-kingdom-uk/ (accessed March 23, 2024).
[51] Busby J. UK shallow ground temperatures for ground coupled heat exchangers. Q J Eng Geol Hydrogeol 2015;48:248–60. https://doi.org/10.1144/QJEGH2015-077.
[52] Ferrari S, Zagarella F, Caputo P, Bonomolo M. Internal heat loads profiles for buildings' energy modelling: comparison of different standards. Sustain Cities Soc 2023;89:104306. https://doi.org/10.1016/J.SCS.2022.104306.
[53] Buildings.fluid.heatexchangers. https://simulationresearch.lbl.gov/modelica/releases/latest/help/Buildings_Fluid_HeatExchangers.html#Buildings.Fluid.HeatExchangers.SensibleCooler_T (accessed October 23, 2023).
[54] Modelica. https://doc.modelica.org/Modelica3.2.3/Resources/helpMapleSim/index.html (accessed October 23, 2023).
[55] Buildings. https://simulationresearch.lbl.gov/modelica/releases/v8.1.0/help/Buildings.html (accessed October 23, 2023).
[56] Jin X, Medina MA, Zhang X. Numerical analysis for the optimal location of a thin PCM layer in frame walls. Appl Therm Eng 2016;103:1057–63. https://doi.org/10.1016/J.APPLTHERMALENG.2016.04.056.
[57] Elarga H, Selvnes H, Sevault A, Hafner A. Numerical investigation of a CO2 cooling system connected to spawn-of-energy-plus thermal zones. Appl Therm Eng 2023;222:119908. https://doi.org/10.1016/J.APPLTHERMALENG.2022.119908.
[58] 8.3 Space heating systems - NHBC Standards 2024. https://nhbc-standards.co.uk/8-services/8-3-space-heating-systems/. 2024, (accessed June 1, 2024).
[59] Global warming set to break key 1.5C limit for first time - BBC News n.d. 2023. https://www.bbc.co.uk/news/science-environment-65602293 (accessed October 23, 2023).
[60] What is energy equality? - Centre for energy equality. https://cee-uk.com/what-is-energy-equality/ (accessed October 23, 2023).
[61] Buildings.boundaryconditions.weatherdata.readerTMY3 (accessed October 24, 2023), https://build.openmodelica.org/Documentation/Buildings.BoundaryConditions.WeatherData.ReaderTMY3.html.